Renewable and Sustainable Energy Reviews 61 (2016) 354–371

Contents lists available at ScienceDirect

Renewable and Sustainable Energy Reviews

journal homepage: www.elsevier.com/locate/rser

Parameter estimation of solar photovoltaic (PV) cells: A review

A. Rezaee Jordehi [1]

Department of Electrical Engineering, Lashtenesha-Zibakenar Branch, Islamic Azad University, Lashtenesha, Iran

ARTICLE INFO

Article history:
Received 29 September 2015
Received in revised form
28 January 2016
Accepted 25 March 2016
Available online 22 April 2016

Keywords:
Solar energy
Solar PV parameter estimation
Photovoltaic systems
Optimisation

ABSTRACT

The contribution of solar photovoltaics (PV's) in generation of electric power is continually increasing. PV cells are commonly modelled as circuits. Finding appropriate circuit model parameters of PV cells is crucial for performance evaluation, control, efficiency computations and maximum power point tracking of solar PV systems. The problem of finding circuit model parameters of solar PV cells is referred to as “PV cell model parameter estimation problem,” and is highly attracted by researchers. In this paper, the existing research works on PV cell model parameter estimation problem are classified into three categories and the research works of those categories are reviewed. Based on the conducted review, some recommendations for future research are provided.

Contents

1. Introduction

In electric power generation, using renewable energy resources instead of conventional fossil-fuelled power generation is exponentially increasing. Among renewable energy resources, solar photovoltaics (PV's) represent the fastest growing resource for electric power generation [1]. They also have the highest power density among all renewable energy resources with global mean of 170 Watt/m^2 [2]. After hydro and wind, solar PV's are the third largest renewable resource of electric power in the world [3,4]. The motivating factors for the replacement of conventional electric power generation by solar PV's are listed out as below.

- Price of fossil fuels is increasing and they may deplete while the source of solar PV's is free and will not run out [5,6].

E-mail address: ahmadrezaeejordehi@gmail.com
[1] Tel.: +98 60129102734.

http://dx.doi.org/10.1016/j.rser.2016.03.049
1364-0321/

- Fossil-fuelled generating units pollute the environment while solar PV's release no pollutant during their operation [7,8].
- Fossil-fuelled generating units contribute to global warming while solar PV's mitigate the global warming issue.
- Unlike fossil-fuelled generating units, the source of solar PV's is omnipresent and abundant.
- Solar PV's have lower maintenance and operational costs [9].
- Among renewables, solar PV's provide the highest power density [2].

Thanks to the above-mentioned advantages, the usage of solar PV's as the source of electrical power is exponentially increasing. Now, more than 100 countries around the globe, are using solar PV's [10]. In order to encourage investments, governments grant financial incentives for solar electricity generation [11–15]. In 2014, the worldwide installed PV electricity was 177 GW and it is expected to be expanded to 220 GW at the end of 2015. This value is around 40 times the installed capacity of 2006 [10]. From the perspective of mounting type, solar PV's may be ground-mounted, integrated into the roof or walls of buildings (building-integrated PV's or BIPV's), rooftop or patio mounting. Solar PV's may work as large-scale centralized power plants or as smaller-scale distributed generation units. Most of solar electricity is generated by solar distributed generation units. PV systems may be connected to the electric grid, which are referred to as grid-connected PV's (GCPV's) and they may work independently which are called standalone PV systems [19–23].

PV cell is the fundamental component of PV systems. Basically, PV cell is a semiconductor diode whose P–N junction is exposed to the light [24]. The physical structure of PV cell has been depicted in Fig. 1.

A thin metallic grid is put on the sun-facing surface of the semiconductor [24]. The size and shape of PV cells are designed in a way that the absorbing surface is maximised and contact resistances are minimised [25]. Several PV cells connected in series form a PV module, some PV modules connected in series and parallel form a PV panel and a PV array may be composed of one or a couple of PV panels. PV systems include solar arrays, DC to DC boost converters and inverters (for grid connected PV systems only) and maximum power point tracking systems. The DC to DC boost converter provides a controllable output voltage. The output voltage and thereby its output power may be controlled by duty cycle of the boost converter. The diagram of a typical PV system has been depicted in Fig. 2.

Despite all the mentioned advantages of solar PV systems, they introduce the following challenges.

- Although PV systems do not produce emissions during their operation, they are not emission-free technologies. In [1], a lifecycle assessment (LCA) of solar PV cells has been done wherein their lifecycle has been divided into three phases; manufacturing, operation and recycling. LCA indicates that manufacturing phase is responsible for most of GHG emissions (around 90 percent) while recycling phase lowers GHG emissions [2,3]. The conducted LCA also indicates that the average lifecycle GHG emissions for solar PV's is 49.9 g CO_2-eq/KW h. In [1], increasing lifespan, increasing capacity factor, using CdTe technology, using ground mounting and installing panels at places with high irradiation have been recommended for decreasing GHG emissions of solar PV systems.

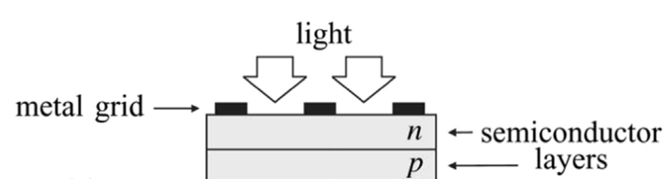

Fig. 1. Physical structure of PV cell [24].

- Currently, the efficiency of solar PV cells is low which increases the cost of their produced electricity. A high amount of research effort is being put to increase the efficiency of solar cells. Low-efficiency solar cells must be recycled and replaced by solar PV cells with higher efficiency [4–7]. In this way, the cost of produced electricity will be decreased.

- A salient challenge of solar PV cells is that how they should be handled after end of their lifecycle. At the end of their life cycle, solar modules and the different parts involved in manufacturing could be recycled. During the recycling process companies can reclaim the semiconductor materials used to build the PV cells, as well as copper, aluminium, glass and other used materials [8]. Once these parts are separated, the reclaimed materials are recycled using the existing recycling methods. Once recycled, solar companies can then employ these materials to build new modules, decreasing their cost of manufacturing [8]. For reducing environmental effects of PV cells, their recycling technology must be expanded and the toxic materials should not be used during the manufacturing of PV cells [8].
- The power generated by solar PV cells is a function of environmental parameters such as irradiation and temperature and therefore is not controllable [16–18]. For mitigating this issue, storage devices are integrated into PV systems.

Appropriate modelling of PV cells is crucial for simulation, design, evaluation, control and optimisation of solar PV systems [27–31]. It is also crucial for efficiency computations and maximum power point tracking of PV systems. Appropriate modelling of PV cells include appropriate circuit model and accurate circuit model parameters. Although, there exist other ways for modelling PV cells, circuit models are the most popular ways for modelling PV cells. Finding the circuit model parameters of PV cells is referred to as "PV cell model parameter estimation problem" and represents a challenging problem in the field of renewable energies. Since, the *I–V* characteristic of PV cells is nonlinear, the PV cell model parameter estimation problem represents a nonlinear optimisation problem. A detailed discussion about the characteristics of PV cell model parameter estimation problem, estimability and identifiability of the model parameters of PV cells is available at [32].

An appropriate parameter estimation method for PV cells should have the following features:

- It should give out accurate model parameters. That is, the model parameters which lead to *I–V* data or remarkable *I–V* points as close as possible to the experimental data or datasheet information.
- It should be robust, that is, when it is applied to a certain dataset for multiple times, very similar results are obtained [33].
- It should provide accurate model parameters for different datasets [33].
- It should have low computational time especially when it is applied for maximum power point tracking.

A great deal of research has already been done to solve "PV cell model parameter estimation problem," however, the research effort is still being put to efficiently solve this problem. In this paper, the existing research works on PV cell parameter estimation problem are reviewed and as per the conducted review, the research gaps are identified and some directions for future research in this field are proposed.

The rest of this paper is organised as follows; in Section 2, different models of PV cells are explained. In Section 3, the problem of parameter estimation of solar PV cells is defined and various strategies for solving this problem are analysed and

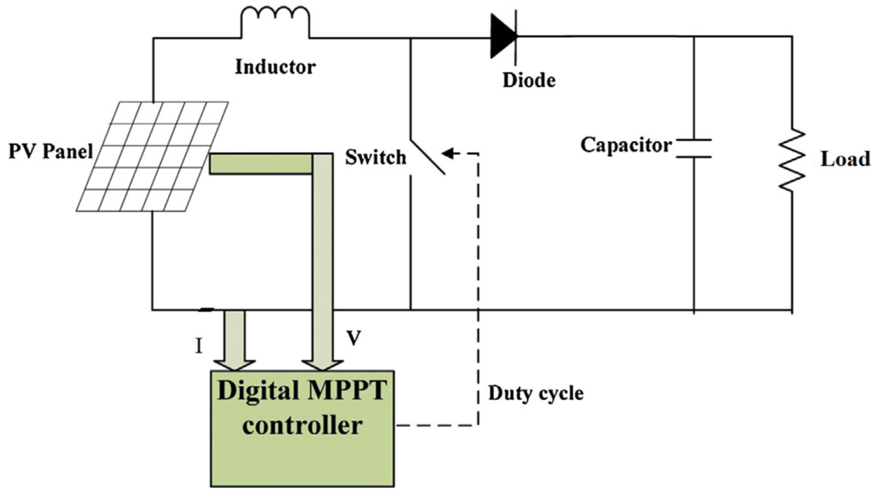

Fig. 2. schematic of a general PV system [26].

reviewed from different point of views. In Section 4, an overall review of different parameter estimation strategies for solar PV's has been provided and some directions for future research are presented. Eventually, the conclusions are provided in Section 5.

2. Models of PV cells

For simulation of PV cells, there exist different approaches. In [34–38] artificial neural networks have been used for modelling the behaviour of PV cells. However, the most common approaches are the ones that model PV cells as circuits [39–59]. In literature, different circuit models for PV cells have been put forward. An appropriate circuit model is the one that accurately emulates the electrical behaviour of physical PV cell and is not too complex. Therefore, a suitable trade-off between accuracy and simplicity must be established during the selection of PV cell circuit model. In this section, various circuit models of PV cells are introduced and analysed.

2.1. Ideal PV cell model

As depicted in Fig. 1, PV cell has two layers of differently doped semiconductor, with its P–N junction exposed to light [25]. Without the presence of solar irradiation, the PV cell functions as a simple P–N junction diode whose I–V curve is given by Shockley equation as below [25].

$$I_D = I_S\left[exp\left(\frac{qV_D}{aKT}\right)-1\right] \tag{1}$$

where I_D and V_D are the current and voltage of diode respectively, I_S is saturation current of diode, a is ideality factor of diode, q is absolute value of electric charge of an electron, T is temperature in Kelvin and K is Boltzman constant.

If the irradiation exists, the P–N junction absorbs the photon from incident light and produces electron-hole pairs (or carriers) [25]. This creates potential difference across the junction, thereby charge carriers start to flow through external circuit [25]. This phenomenon is referred to as photovoltaic effect and the resulting electrical current is named photocurrent and denoted by I_{PV} [25]. The addition of I_{PV} into Shockley equation forms an elementary description of an illuminated PV cell that includes a current source paralleled by a P–N junction diode [25]. The resultant circuit is referred to as ideal PV cell model and is depicted as Fig. 3. As Fig. 4 indicates, I is the superposition of I_{PV} and I_D. It is evident that the mentioned ideal PV cell model has three parameters; I_{PV}, a and I_S.

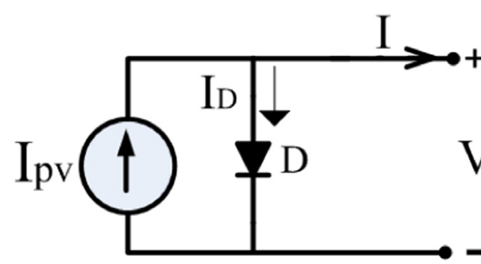

Fig. 3. Ideal model of PV cell.

Fig. 5 shows three remarkable points of I–V curve of PV cells that are published by PV manufacturers.

The generated photocurrent is very sensitive to environmental conditions and can be represented by the following equation.

$$I_{PV}(T,G) = \left(I_{PV,STC} + K_I(T-T_{STC})\right)\frac{G}{G_{STC}} \tag{2}$$

where $I_{PV,STC}$, T_{STC} and G_{STC} represent the values of photocurrent, temperature and irradiation at standard test conditions (STC). At STC, the temperature is 25° of centigrade, the irradiation is 1000 W/m^2 and air mass is 1.5. Symbols T and G respectively represent temperature and irradiation at which the photocurrent is computed. K_I represents temperature coefficient of photocurrent. Since during short circuit, diode current may be neglected in comparison with generated photovoltaic current, the photovoltaic current and short circuit current may be taken approximately equal. Short circuit current is denoted by I_{SC}.

The I–V characteristic of ideal PV cell model can be represented by Eq. (3).

$$I = I_{PV} - I_S\left[exp\left(\frac{qV}{aKT}\right)-1\right] \tag{3}$$

The open circuit voltage, voltage and current at maximum power of PV cell are also functions of the temperature and irradiation as follows [60,61].

$$V_{OC}(T,G) = V_{OC,STC} + K_V(T-T_{STC}) + V_t Ln\left(\frac{G}{G_{STC}}\right) \tag{4}$$

$$V_{mp}(T,G) = V_{mp,STC} + K_V(T-T_{STC}) + V_t Ln\left(\frac{G}{G_{STC}}\right) \tag{5}$$

$$I_{mp}(T,G) = \left(I_{mp,STC} + K_I(T-T_{STC})\right)\frac{G}{G_{STC}} \tag{6}$$

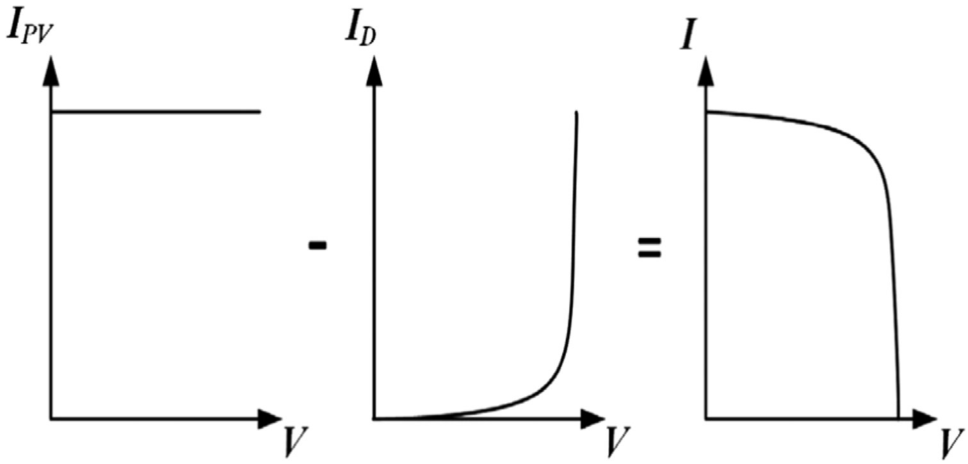

Fig. 4. I as superposition of I_{PV} and I_D [24,25].

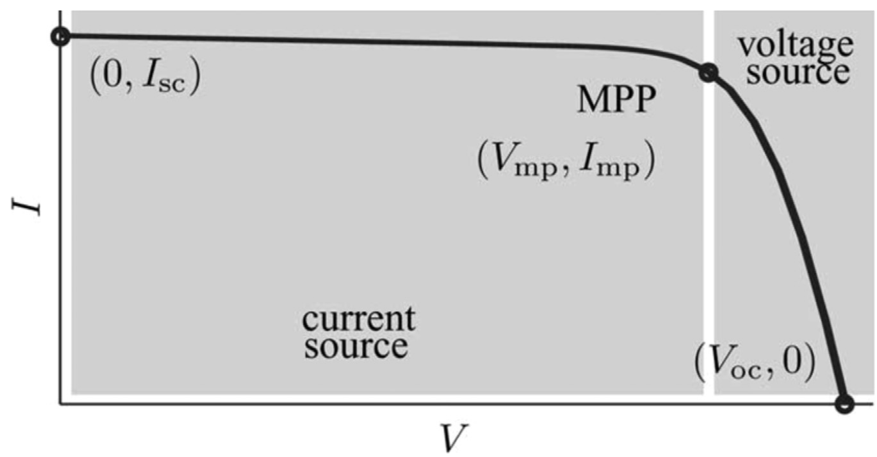

Fig. 5. Three remarkable points of $I-V$ curve of PV cell [24].

where K_V and K_I represent temperature coefficient of voltage and current respectively, V_{OC} denotes open circuit voltage, V_{mp} and V_{mp} respectively represent voltage and current at maximum power. Finally V_t represents thermal voltage of diode. It is defined by multiplication of ideality factor, Boltzman constant and temperature divided by the absolute charge of electron.

Normally, PV manufacturers publicise the values of V_{OC} , I_{SC} , V_{mp}, I_{mp} , K_I and K_V . All data are published for standard test condition. Ideal PV cell model is only used to explain fundamental concepts of PV cells and is not used for simulation of PV cells, since it can not emulate the behaviour of physical PV cells.

2.2. Single diode R_S model

As mentioned in the previous subsection, the ideal single diode model is not used in PV simulations and is merely used to explain theoretical concepts of PV cells [25,62,63]. To introduce a more realistic model for PV cells, the contact resistance between silicon and electrodes surfaces, the resistance of electrodes and the current flow resistance are taken into account and modelled as a series resistance denoted by R_S [25]. The model of single diode R_S model has been depicted in Fig. 6. It has four parameters; I_{PV}, a , I_S and R_S. Its $I–V$ characteristic is given by Eq. (7). Although single diode R_S model imitates the behaviour of physical PV cells, better than ideal PV cell model, its modelling accuracy is not enough.

$$I = I_{PV} - I_S\left[exp\left(\frac{q(V+R_SI)}{aKT}\right) - 1\right] \tag{7}$$

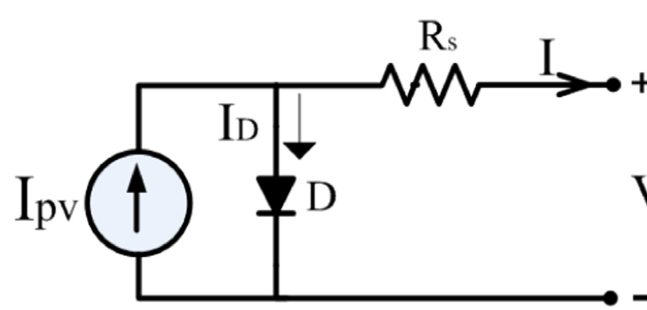

Fig. 6. Single diode R_S model.

2.3. Single diode R_P model

In order to take the leakage current of P–N junction into account, a shunt resistance R_P is added to the PV cell model. The resultant model is referred to as single diode R_P model and is the most commonly used PV cell model thanks to its relatively appropriate tradeoff between accuracy and simplicity. Nonetheless, its accuracy in low values of irradiation is not acceptable. Single diode R_P model has five parameters; I_{PV}, a , I_S , R_S and R_P . The model of single diode R_P model has been depicted in Fig. 7 and its $I–V$ characteristic is given by Eq. (8).

$$I = I_{PV} - I_S\left[exp\left(\frac{q(V+R_SI)}{aKT}\right) - 1\right] - \frac{V+R_SI}{R_P} \tag{8}$$

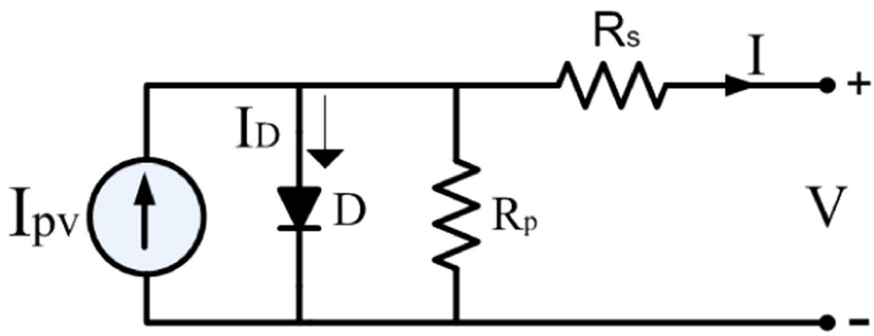

Fig. 7. Single diode R_P model.

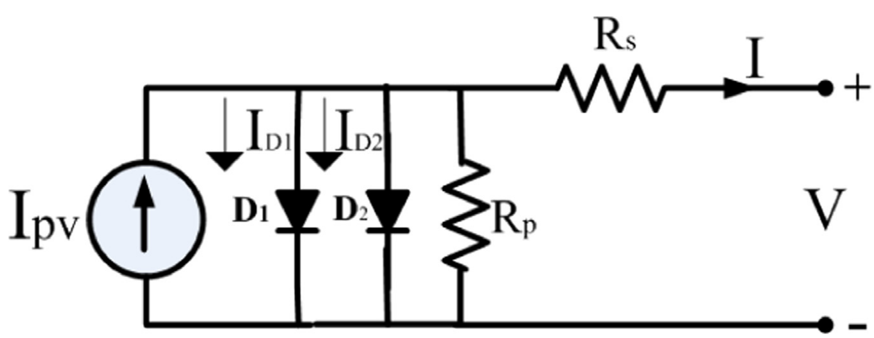

Fig. 8. Two diode model for PV cell.

It should be noted here that all parameters of PV cell model are dependent on environmental conditions. The dependence of photocurrent to environmental conditions was characterised by Eq. (2). Dependence of other PV cell parameters on environmental conditions can be represented by the following equations [4].

$$I_S(T,G) = I_{S,STC}\left(\frac{T}{T_{STC}}\right)^3 exp\left(\frac{E_g}{K}\left(\frac{1}{T_{STC}} - \frac{1}{T}\right)\right) \tag{9}$$

$$R_S(T,G) = R_{S,STC}\frac{T}{T_{STC}}\left(1 - 0.217ln\frac{G}{G_{STC}}\right) \tag{10}$$

$$R_P(G) = R_{P,STC}\frac{G_{STC}}{G} \tag{11}$$

$$a(T) = a_{STC}\frac{T}{T_{STC}} \tag{12}$$

where E_g is the material's energy band gap, $I_{S,STC}$, $R_{S,STC}$, $R_{P,STC}$ and a_{STC} are respectively diode's saturation current, series resistance, shunt resistance and diode's ideality factor at standard test conditions.

2.4. Two diode model

Taking the effect of recombination current loss in the depletion region into account, the second diode (D_2) is added to the model of PV cell. The advantage of this model is that unlike the single diode models, it provides appropriate accuracy in low irradiation values. Two diode model has seven parameters; I_{PV} , R_S , R_P , a and I_S of the first diode, a and I_S of the second diode. The model of two diode model has been depicted in Fig. 8 and its I–V characteristic is given by Eq. (13) [64–66].

$$I = I_{PV} - I_{S_1}\left[exp\left(\frac{q(V+R_SI)}{a_1KT}\right) - 1\right] - I_{S_2}\left[exp\left(\frac{q(V+R_SI)}{a_2KT}\right) - 1\right] - \frac{V+R_SI}{R_P} \tag{13}$$

2.5. Other PV cell models

Besides the above-mentioned models, some other models for PV cells have been introduced in the literature. Single diode model with capacitance [67], three diode model [68], modified two diode models [69,70], drift-diffusion model [71] and multi-dimension diode model [72] are some examples of those models. However, generally due to the complexity of these models, their application in simulation of PV cells is very limited.

3. Parameter estimation of PV cells

PV cell manufacturers generally provide values of V_{OC}, I_{SC}, P_{mp}, K_I and K_V . The data are published for standard test condition. For simulating PV cells, first a suitable model must be selected considering an appropriate tradeoff between accuracy and simplicity. After selecting an appropriate model, circuit model parameters must be determined, since model parameters are required for simulation of PV cells and arrays. The problem of finding PV cell model parameters based on datasheet information or experimental I–V data is referred to as “PV cell model parameter estimation problem.” Thanks to the fact that the accuracy of values of PV cell model parameters affect efficiency and maximum power point tracking computations, finding model parameters that provide high accuracy in simulations, is of very high importance and significance. As a result, this problem has been highly attracted by researchers.

For determining PV cell model parameters, different methodologies have been proposed in the literature. All those methodologies can be classified into three main categories. The first category of methodologies include analytical methods that provide formulations for deriving model parameters based on datasheet information or I–V curve data. The second category of methodologies translate PV cell model parameter estimation problem into an optimisation problem. The values of model parameters form the decision vector of optimisation problem and its objective is minimisation of error-based metrics. The resultant optimisation problem is solved by metaheuristic optimisation algorithms. The third category of methodologies are hybrids of analytical and metaheuristic approaches, meaning that some model parameters are computed by an analytical approach and the remaining set of model parameters are found by metaheuristic optimisation algorithms. In this section, the research works of these three categories are analysed.

3.1. Analytical methods for parameter estimation of PV cells

In a large number of research works, analytical methods have been used to extract model parameters of PV cells. In this section, those research work are classified based on their used PV cell model and will be analysed.

3.1.1. Analytical methods for parameter estimation of single diode R_S models

As stated in Section 2.2, Single diode R_S model has four parameters; I_{PV}, a , I_S and R_S . For extracting the values of these four parameters, four equations are required [73,74]. Normally, PV manufacturers publicise the values of V_{OC} , I_{SC} , V_{mp}, I_{mp} , K_I and K_V. In some cases, the *I*–*V* curve or the solpes of *I*–*V* curve at open circuit point and short circuit point are available. The reciprocal of absolute solpe of *I*–*V* curve at open circuit point is denoted by R_{S0} and the reciprocal of its aboute slope at short circuit point is denoted by R_{P0} . The four required equations may be provided by the following two ways (either using Eqs. (19)–(21), (25) or using Eqs. (19)–(21), (26)).

Based on Eq. (7), at open circuit point, we have:

$$0=I_{PV}-I_S\left[exp\left(\frac{q(V_{OC})}{aKT}\right)-1\right] \tag{14}$$

Therefore,

$$I_{PV}=I_S\left[exp\left(\frac{q(V_{OC})}{aKT}\right)-1\right] \tag{15}$$

Based on Eq. (7), at short circuit point, we have:

$$I_{SC}=I_{PV}-I_S\left[exp\left(\frac{qR_SI_{SC}}{aKT}\right)-1\right] \tag{16}$$

By reforming Eq. (16), we have:

$$I_{PV}=I_{SC}+I_S\left[exp\left(\frac{qR_SI_{SC}}{aKT}\right)-1\right] \tag{17}$$

From (15) and (17), we have

$$I_S\left[exp\left(\frac{q(V_{OC})}{aKT}\right)-1\right]=I_{SC}+I_S\left[exp\left(\frac{qR_SI_{SC}}{aKT}\right)-1\right] \tag{18}$$

Therefore, saturation current as a model parameter can be computed by

$$I_S=\frac{I_{SC}}{exp\left(\frac{q(V_{OC})}{aKT}\right)-exp\left(\frac{qR_SI_{SC}}{aKT}\right)} \tag{19}$$

By pluging (19) into (17), photocurrent can be computed by:

$$I_{PV}=I_{SC}\left[1+\frac{I_{SC}\left(exp\left(\frac{qR_SI_{SC}}{aKT}\right)-1\right)}{exp\left(\frac{q(V_{OC})}{aKT}\right)-exp\left(\frac{qR_SI_{SC}}{aKT}\right)}\right] \tag{20}$$

It should be noted that in some cases, the diode current at short circuit point is neglected, thereby I_{PV} and I_{SC} are taken equal [75–77].

Based on Eq. (7), at maximum power point, we have

$$I_{mp}=I_{PV}-I_S\left[exp\left(\frac{q(V_{mp}+R_SI_{mp})}{aKT}\right)-1\right] \tag{21}$$

Since the derivative of output power with respect to voltage at maximum power point must be zero:

$$\frac{dP}{dV}=\frac{d(VI)}{dV}=V\frac{dI}{dV}+I=0 \tag{22}$$

From (22), it is concluded that at maximum power point we have:

$$\frac{dI}{dV}=\frac{-I_{mp}}{V_{mp}} \tag{23}$$

By differentiating *I* with respect to *V* in Eq. (7), we have:

$$\frac{\mathrm{dI}}{\mathrm{dV}}=\frac{\left[\frac{\mathrm{qI_S}}{\mathrm{aKT}}exp\left(\frac{q(V+R_SI)}{aKT}\right)\right]}{\left[\frac{\mathrm{qR_S}}{\mathrm{aKT}}exp\left(\frac{q(V+R_SI)}{aKT}\right)-1\right]} \tag{24}$$

From (23) and (24), we extract Eq. (25).

$$\frac{\left[\frac{\mathrm{qI_S}}{\mathrm{aKT}}exp\left(\frac{q(V_{mp}+R_SI_{mp})}{aKT}\right)\right]}{\left[\frac{\mathrm{qR_S}}{\mathrm{aKT}}exp\left(\frac{q(V_{mp}+R_SI_{mp})}{aKT}\right)-1\right]}=\frac{-I_{mp}}{V_{mp}} \tag{25}$$

The slope of *I*–*V* curve at short circuit point can be used to derive another equation.

$$\frac{\frac{\mathrm{qI_S}}{\mathrm{aKT}}exp\left(\frac{qR_SI_{SC}}{aKT}\right)}{\left[\frac{\mathrm{qR_S}}{\mathrm{aKT}}exp\left(\frac{qR_SI_{SC}}{aKT}\right)-1\right]}=\frac{-1}{R_{S0}} \tag{26}$$

In Table 1, the way that the four required equations in single diode R_S models are extracted, will be explained.

3.1.2. Analytical methods for parameter estimation of single diode R_P models

As stated in Section 2.3, single diode R_P model has five parameters; I_{PV}, a , I_S $R_S$and R_P [81]. For extracting the values of these five parameters, five equations are required. Five equations among the following set of equations are used for extraction of model parameters.

First of all, in some cases, the ideality factor of the diode is arbitrarily chosen in the range [1, 2.5].

Based on Eq. (8), at open circuit point, we have:

$$0=I_{PV}-I_S\left[exp\left(\frac{qV_{OC}}{aKT}\right)-1\right]-\frac{V_{OC}}{R_P} \tag{27}$$

Therefore, we can write:

$$I_{PV}=I_S\left[exp\left(\frac{qV_{OC}}{aKT}\right)-1\right]+\frac{V_{OC}}{R_P} \tag{28}$$

Table 1
Ways of extraction of equations in single diode R_S models.

Ref	Equations
[75,78]	Short circuit point, open circuit point, slope of *I*–*V* curve at open circuit point, ideality factor of diode is arbitrarily chosen in [1,2].
[73]	Short circuit point, open circuit point, maximum power point, the derivative of power with respect to voltage at maximum power point is set to zero.
[79]	Short circuit point, open circuit point, maximum power point, the derivative of power with respect to voltage at maximum power point is set to zero.
[80]	Short circuit point, open circuit point, maximum power point, the derivative of power with respect to voltage at maximum power point is set to zero.

Based on Eq. (8), at short circuit point, we have:

$$I_{SC}=I_{PV}-I_S\left[exp\left(\frac{qR_SI_{SC}}{aKT}\right)-1\right]-\frac{R_SI_{SC}}{R_P} \tag{29}$$

Therefore, we have:

$$I_{PV}=I_{SC}+I_S\left[exp\left(\frac{qR_SI_{SC}}{aKT}\right)-1\right]+\frac{R_SI_{SC}}{R_P} \tag{30}$$

By equating (28) and (30), we have:

$$I_S\left[exp\left(\frac{qV_{OC}}{aKT}\right)-1\right]+\frac{V_{OC}}{R_P}=I_{SC}+I_S\left[exp\left(\frac{qR_SI_{SC}}{aKT}\right)-1\right]+\frac{R_SI_{SC}}{R_P} \tag{31}$$

Therefore, we have:

$$I_S=\frac{I_{SC}+\frac{R_SI_{SC}}{R_P}-\frac{V_{OC}}{R_P}}{exp\left(\frac{qV_{OC}}{aKT}\right)-exp\left(\frac{qR_SI_{SC}}{aKT}\right)} \tag{32}$$

Then, by inserting (32) in (28), we have:

$$I_{PV}=\frac{\left(I_{SC}+\frac{R_SI_{SC}}{R_P}-\frac{V_{OC}}{R_P}\right)\left(exp\left(\frac{qV_{OC}}{aKT}\right)-1\right)}{exp\left(\frac{qV_{OC}}{aKT}\right)-exp\left(\frac{qR_SI_{SC}}{aKT}\right)}-\frac{V_{OC}}{R_P} \tag{33}$$

Based on Eq. (8) at maximum power point, we have:

$$I_{mp}=I_{PV}-I_S\left[exp\left(\frac{q(V_{mp}+R_SI_{mp})}{aKT}\right)-1\right]-\frac{V_{mp}+R_SI_{mp}}{R_P} \tag{34}$$

By differentiating I with respect to V in Eq. (8), we have:

$$\frac{dI}{dV}=\frac{-\left[\frac{qI_S}{aKT}exp\left(\frac{q(V+R_SI)}{aKT}\right)+\frac{1}{R_P}\right]}{\left[\frac{R_SI_S}{aKT}exp\left(\frac{q(V+R_SI)}{aKT}\right)+\frac{R_S}{R_P}+1\right]} \tag{35}$$

Then using Eq. (23), at maximum power point, we have:

$$\frac{-\left[\frac{qI_S}{aKT}exp\left(\frac{q(V_{mp}+R_SI_{mp})}{aKT}\right)+\frac{1}{R_P}\right]}{\left[\frac{R_SI_S}{aKT}exp\left(\frac{q(V_{mp}+R_SI_{mp})}{aKT}\right)+\frac{R_S}{R_P}+1\right]}=\frac{-I_{mp}}{V_{mp}} \tag{36}$$

The slope of I–V curve at short circuit point (R_{S0}) can be used to derive another equation.

$$\frac{-\left[\frac{qI_S}{aKT}exp\left(\frac{qR_SI_{SC}}{aKT}\right)+\frac{1}{R_P}\right]}{\left[\frac{R_SI_S}{aKT}exp\left(\frac{qR_SI_{SC}}{aKT}\right)+\frac{R_S}{R_P}+1\right]}=\frac{-1}{R_{S0}} \tag{37}$$

Similarly, the slope of I–V curve at open circuit point (R_{P0}) can be used to derive another equation.

$$\frac{-\left[\frac{qI_S}{aKT}exp\left(\frac{qV_{OC}}{aKT}\right)+\frac{1}{R_P}\right]}{\left[\frac{R_SI_S}{aKT}exp\left(\frac{qV_{OC}}{aKT}\right)+\frac{R_S}{R_P}+1\right]}=\frac{-1}{R_{P0}} \tag{38}$$

In some cases, R_P and R_{P0} have been assumed equal [82,83].

In Table 2, data used for extracting the five required equations in single diode R_P models, will be explained. Interested reader can also refer to previous review's on analytical methods in parameter estimation of solar PV cells [33,84–87].

In [62], five different analytical PV cell parameter extraction methods including [24,83,89,90,95] have been compared. From the perspective of availability of required data, [83,89,90] need the slope of I–V curve at short circuit and open circuit points which are not commonly available, or [95] requires a graphical estimation of slope of I–V curve at maximum power point and also slope of I–V curve at open circuit point which are not commonly available. However, in [24], the required data are available in literature and does not require any graphical estimation of I–V curve of PV cell. The comparative results at different irradiations and temperatures indicate that [90] provides the best performance and suitably emulates the performance of physical PV cells.

Table 2
Information used for preparation of equations in single diode R_P models.

Ref.	Equations
[4]	V_{OC} , I_{SC} , $\frac{dP}{dV}=0$, R_{P0} , R_{S0}
[88]	V_{OC} , I_{SC} , V_{mp}, I_{mp}, R_{P0} , R_{S0}
[83]	V_{OC} , I_{SC} , V_{mp}, I_{mp}, R_{S0} , R_{P0}
[89]	V_{OC} , I_{SC} , V_{mp}, I_{mp}, R_{S0} , R_{P0}
[90]	V_{OC} , I_{SC} , V_{mp}, I_{mp}, R_{S0} , R_{P0}
[91]	V_{OC} , I_{SC} , V_{mp}, I_{mp}, R_{S0} , R_{P0}
[92]	V_{OC} , I_{SC} , V_{mp}, I_{mp}, , R_{P0} , $\frac{dP}{dV}=0$
[82]	V_{OC} , I_{SC} , V_{mp}, I_{mp}, R_{S0} , R_{P0}
[93]	V_{OC} , I_{SC} , V_{mp}, I_{mp}, R_{S0} , a is arbitrarily chosen in [1,2].
[94]	V_{OC} , I_{SC} , V_{mp}, I_{mp}, , $\frac{dP}{dV}=0$, a is set as 1.

3.1.3. Analytical methods for parameter estimation of two diode models

As mentioned in section 2.4, two diode model has seven parameters; I_{PV} , R_S , R_P , a and I_S of the first diode, a and I_S of the second diode. In order to identify these seven parameters, seven equations are required. Three equations are derived by using I–V characteristic of Eq. (13) at short circuit point, open circuit point and maximum power point. The slope of I–V curve at short circuit point and open circuit point lead to two other equations. The derivative of power with respect to voltage at maximum power point is set to zero to extract the sixth equation and eventually sum of ideality factors of two diodes are set to 3 to derive the seventh equation [96–100].

Critically speaking about analytical parameter estimation approaches for PV cells, the following points must be pointed out.

- In most of cases, the resultant algebraic equations are transcendent that are very difficult to be solved.
- In some cases, the initial estimates of parameters are needed.
- Some of them are based on the data which are not available in practice, that is, those data are not provided by PV manufacturers.
- In most of cases, simplifying assumptions are used that reduce the accuracy of the model parameters.
- In some cases, they suffer from convergence problem.

3.2. Metaheuristics for parameter estimation of PV cells

PV cell model parameter estimation problem can be easily translated into an optimisation problem. The resultant optimisation problem is nonlinear, constrained and continuous and represents a difficult optimisation problem. Metaheuristic optimisation algorithms are very common in solving difficult Engineering optimisation problems [101–108]. They are probabilistic, population-based optimisation algorithms that commonly take inspiration from nature and have proved to be efficient in solving difficult Engineering optimisation problems. They do not require convexity, continuity or differentiability of objective functions. In the last decade, metaheuristics have been frequently applied for parameter estimation of circuit model parameters of solar PV cells. In this subsection, the application of metaheuristics in parameter estimation of circuit model of solar PV cells will be reviewed.

In [1], artificial bee colony (ABC) has been used for estimating parameters of single and double diode models. ABC has taken inspiration from food foraging behaviour of bees [109]. Experimental I–V data from [110] has been used for parameter estimation. Normalised value of $RMSE$ (root mean square error) has been selected as objective functions. It is defined as below.

$$RMSE = \sqrt{\frac{\sum_{i=1}^{N} (I_{i,exp} - I_{i,est})^2}{N}} \quad (39)$$

where $I_{i,exp}$ represents ith experimental current of PV cell, $I_{i,est}$ represents ith estimated current of PV cell and N is the number of I–V points. For parameter estimation of single diode model, the decision vector is as follows:

$$X = [I_{PV}, I_S, a, R_S, R_P] \quad (40)$$

For parameter estimation of double diode model, the decision vector is as bellow:

$$X = [I_{PV}, I_{S1}, a_1, I_{S2}, a_2, R_S, R_P] \quad (41)$$

The decision variables are bounded in the ranges below.

$R_S \in [0, 0.5]\Omega$, $R_P \in [0, 100]\Omega$, $I_{PV} \in [0, 1]$A, $I_S \in [0, 1]\mu$A, $a \in [1, 2]$.

The results have been obtained for five different temperatures in 57 mm diameter commercial silicon solar cell (RTC France). The results approve the outperformance of the ABC algorithm over harmony search (HS), particle swarm optimisation (PSO), genetic algorithm (GA) and bacterial foraging optimisation algorithm (BFOA). The outperformance is both in terms of accuracy and robustness.

In [27], a modified version of artificial bee colony (ABC) [111] has been used for estimating parameters of single and double diode models. Twenty six pairs of experimental I–V data from [110] has been used. Since experimental data contain noise, the resultant objective function is noisy [1,112–114]. For parameter estimation of single and double diode model, the decision vectors are the same as (40) and (41) respectively. The decision variables are bounded within the ranges below.

$R_S \in [0, 0.5]\Omega$, $R_P \in [0, 100]\Omega$, $I_{PV} \in [0, 1]$A, $I_S \in [0, 1]\mu$A, $a \in [1, 2]$

The results have been obtained for 57 mm diameter commercial silicon solar cell (RTC France). The proposed modified ABC outperforms GA, simulated annealing (SA), pattern search (PS), harmony search (HS) and chaotic PSO. The results show that the difference between single diode and double diode models is only 0.79% that indicates the suitability of single diode model.

Differential evolution (DE) is an evolutionary optimisation algorithm mainly based on differential mutation operator and crossover operator [115]. DE is considered as a powerful optimisation algorithm in solving difficult optimisation problems [116]. In [117], an adaptive version of DE has been used for parameter estimation of single diode model of PV cells based on datasheet information. In the proposed adaptive DE, scaling factor (F) and crossover rate (CR) as control parameters of DE are adaptively controlled during the course of run. This adaptation emulates the attraction and repulsion phenomena of electromagnetism. $RMSE$ defined by (39) is the objective function. The decision variables are bounded in the ranges below.

$R_S \in [0.1, 2]\Omega$, $R_P \in [100, 5000]\Omega$, $I_{PV} \in [1, 8]$A, $I_S \in [1e-12, 1e-5]\mu$A, $a \in [1, 2]$

Although datasheet information have been used for estimation of model parameters, experimental I–V data has been used for validation of estimated parameters. Model parameters have been separately extracted for seven different irradiation values. The findings approve the outperformance of the proposed adaptive DE over penalty-based DE [118] and an analytical approach.

In [118], penalty function approach has been incorporated into DE in order to handle constraints. It penalises infeasible search agents based on their amount of constraint violations. DE/best/1/bin has been used wherein 1 represents the number of mutation vectors and "bin" represents binomial crossover. The proposed penalty-based DE has been used to estimate parameters of two diode model using synthetic data. $RMSE$ defined by (39) is the objective function. The decision variables are bounded in the ranges below.

$R_S \in [0, 1]\Omega$, $R_P \in [50, 1000]\Omega$, $I_{PV} \in [0, 7.6]$A,
$I_{S1} \in [1e-12, 1e-5]\mu$A, $a_1 \in [0.5, 4]$, $I_{S2} \in [1e-12, 1e-5]\mu A$,
$a_2 \in [0.5, 4]$, $I_{S2} \in [2, 7]I_{S1}$

First, synthetic data from two diode model with the following parameters are generated.

$R_S = 0.32\Omega$, $R_P = 200\Omega$, $I_{PV} = 3.8$A, $I_{S1} = 4.7e-10\mu$A, $a_1 = 1$,
$I_{S2} = 2.11e-6\mu$A, $a_2 = 2$

Then, the penalty-based DE is used to extract model parameters from synthetic data. The results on six solar modules of different types including multi-crystalline, mono-crystalline and thin-film indicate the outperformance of the proposed penalty-based PSO over GA, SA and PSO. The proposed penalty-based DE performs well in all terms of accuracy, consistency and convergence speed.

In [119], another adaptive variant of DE has been introduced wherein adaptive strategies have been proposed for scaling factor and crossover rate. In the proposed adaptive DE, at each iteration, the value of A is computed by

$$A = \frac{best\ fitness(t)}{best\ fitness(t-1)} \quad (42)$$

where $bestfitness(t)$ and $bestfitness(t-1)$ respectively represent the best fitness at iterations t and $t-1$ respectively. Then scaling factor and crossover rate are computed by:

$$F = 0.5exp(ln(2).r_1.A) \quad (43)$$

$$CR = 0.5exp(ln(2).r_2.A) \quad (44)$$

where r_1 and r_2 are two random numbers in [0, 1].

With the proposed adaptive strategy, characterised by Eqs. (42)–(44), if the best fitness value does not improve over a iteration, the values of scaling factor and crossover rate are adjusted in a way that the diversity among search agents is increased.

The proposed adaptive DE has been applied to parameter estimation problem of solar PV cells. Parameter estimation has been done for single diode model. Both Synthetic and experimental data have been used. $RMSE$ defined by (39) is the objective function. The decision variables are bounded in the ranges below.

$R_S \in [0, 2]\Omega$, $R_P \in [50, 5000]\Omega$, $I_{PV} \in [0, 5]$A, $I_S \in [1e-12, 1e-5]$ μA, $a \in [0.5, 10]$

In this work, the upper range for ideality factor of diode seems unusual.

An important advantage of the proposed adaptive DE is that it does not require the tuning of any control parameter. The results approve the outperformance of the proposed adaptive DE over PSO, GA, conventional DE, SA and an analytical approach.

In [120], an improved version of JADE [121], referred to as "repaired adaptive JADE" has been applied to parameter estimation problem of solar PV cells. In this improved algorithm, a repaired adaptive crossover rate, an adaptive strategy for scaling factor and a ranking-based mutation strategy is used. In the proposed mutation strategy, fitter individuals will have higher chance to be involved in mutation operation. The range of decision variables are as follows.

$R_S \in [0, 0.5]\Omega$, $R_P \in [0, 100]\Omega$, $I_{PV} \in [0, 1]$A, $I_S \in [0, 1]\mu$A, $a \in [1, 2]$

The parameters of both single and double diode models have been estimated using experimental data. Again, $RMSE$ has been used as objective function. The results have been obtained for 57 mm diameter commercial silicon solar cell (RTC France). The proposed modified JADE outperforms PSO, SA, ABC [27], HS, pattern search (PS), Newton, JADE and some other DE variants.

Particle swarm optimisation (PSO) is a leader-based metaheuristic wherein each particle is both attracted by its own best search experience, named as personal best and the best search experience of the swarm, named as global best [122–125]. The effect of personal bests and global best can be respectively adjusted by cognitive and social acceleration coefficients [126,127]. Cognitive and social acceleration coefficients along with inertia weight are control parameters that may significantly affect the performance of PSO. PSO is a very popular metaheuristic for solving real-world optimisation problems [103,128–130].

In [131], linearly decreasing inertia weight PSO with equal values of cognitive and social acceleration coefficients has been used for parameter estimation of two diode and three diode models via datasheet information. In the proposed PSO, the velocity of particles are bounded within a specified range. The objective function is mean absolute error metric defined by the following equation.

$$MAE = \frac{\sum_{i=1}^{N} (I_{i,exp} - I_{i,est})}{N} \tag{45}$$

As expected, the findings show that the three diode model provides more accurate parameters than two diode model. Normally, in three diode model, the number of decision variables in model parameter estimation problem should be 9, however, in this research work, photocurrent is assumed equal to short circuit current and the ideality factors of the first and second diodes are respectively assumed as 1 and 2, therefore the number of decision variables is reduced to 6. The proposed PSO has outperformed DE.

In [132,133], Pattern search [134,135] has been used for parameter estimation of PV cells with single diode model. Experimental *I–V* data has been used for parameter estimation. The objective function is defined as below.

$$OF = \sum_{i=1}^{N} abs(I_{i,exp} - I_{i,est}) \tag{46}$$

The findings show that pattern search outperforms GA, Newton method [110,136].

In [137], biogeography-based optimisation (BBO) with mutation strategy has been used for parameter estimation of single and double diode models. BBO takes inspiration from biogeographic species [138–140]. The mutation strategy is adopted from DE and chaos theory. Logistic map function has been used as chaotic function [141–143]. Again, *RMSE* has been used as objective function and ranges of decision variables have been set as below.

$$R_S \in [0, 0.5]\Omega,\ R_P \in [0, 100]\Omega,\ I_{PV} \in [0, 1]\text{A},\ I_S \in [0, 1]\mu\text{A}, a \in [1, 2]$$

The proposed mutation-integrated BBO provides desirable accuracy and convergence speed. It outperforms an intensive set of optimisation algorithms including conventional BBO, PSO, GA, DE, PS, ABC, SA, HS and chaotic PSO.

In [144], innovative global harmony search (IGHS) as a modified version of HS has been proposed for parameter estimation of single and double diode models. In IGHS, a predefined number of harmonies with the best fitness values are selected as elite harmonies. Then, a probabilistic roulette wheel is used to select one of them for improvisation process. In this way, the probability of generating harmonies of high quality is increased and more accurate solution can be found. Twnty six pairs of experimental *I–V* data from [110] has been used. Again, *RMSE* is the objective function and ranges of decision variables are set as follows.

$$R_S \in [0, 0.5]\Omega,\ R_P \in [0, 100]\Omega,\ I_{PV} \in [0, 1]\text{A},\ I_S \in [0, 1]\mu\text{A},\ a \in [1, 2]$$

The results testify that the proposed innovative global harmony search (IGHS) outperforms conventional HS, SA and PS.

In [145], simulated annealing (SA) has been used for estimating parameters of single and double diode models via experimental *I–V* data. SA is inspired from annealing process of materials in metallurgy [146,147]. Objective function is the same with (46). The findings approve that SA outperforms [136,110].

In [148], bird mating optimisation (BMO) inspired from mating strategies of bird species has been used for parameter estimation of solar PV cells via experimental *I–V* data. Parameters have been estimated for both single and double diode models. *RMSE* is the objective function and ranges of decision variables are as below.

$$R_S \in [0, 0.5]\Omega,\ R_P \in [0, 100]\Omega,\ I_{PV} \in [0, 1]\text{A},\ I_S \in [0, 1]\mu\text{A},\ a \in [1, 2]$$

The results indicate that BMO outperforms PS, SA, HS, ABC, PSO, GA and IGHS [144].

In [149], flower pollination algorithm has been used for parameter estimation of solar PV cells via experimental *I–V* data. flower pollination algorithm emulates the pollination performance of flowers [150–152]. Parameter estimation has been done for both single and double diode models. *RMSE* is the objective function. The achieved results demonstrate the superiority of flower pollination algorithm over Newton method [110], BFOA, DE, HS, ABC, PS, hybrid GA-interior point [153], parallel chaos optimisation [154] and cuckoo search optimisation (CSO) algorithm. The outperformance is both in terms of accuracy and convergence speed.

In [155], a modified version of teaching-learning based optimisation (TLBO) [102,156,157] algorithm has been used for parameter estimation of solar PV cells via experimental *I–V* data. TLBO is a metaheuristic optimisation algorithm that emulates the performance of teachers and students in classroom. The algorithm includes two different phases; teaching phase and learning phase. *RMSE* is the objective function. In the proposed version of TLBO, the learner phase has not been changed, while the teacher phase has been modified. In teaching phase, a local search operator is incorporated in order to enhance the global best and an elite strategy is used to update the current worst learner. The local search is done with the following equation.

$$global\ best = \begin{cases} global\ best + mu & if\, r < \mu \\ global\ best & \text{otherwise} \end{cases} \tag{47}$$

where *mu* represents the step size of local search and μ denotes its probability. Symbol r denotes a random number in [0, 1].

The step size of local search operator is computed via logistic chaotic map function. Via the local search, the global best of individuals is enhanced during the course of the run. The ranges of decision variables have been set as below.

$$R_S \in [0, 0.5]\Omega,\ R_P \in [0, 100]\Omega,\ I_{PV} \in [0, 1]\text{A},\ I_S \in [0, 1]\mu\text{A},\ a \in [1, 2]$$

The results indicate that the proposed modified TLBO outperforms conventional TLBO, ABC [27], innovative global harmony search [144], PS and SA. The outperformance is both in terms of accuracy and convergence speed. The salient disadvantage of the proposed TLBO variant is that unlike conventional TLBO that introduces no control parameter, it introduces mutation probability as a control parameter which must be tuned by user.

In [154], a modified version of population-based chaos optimisation algorithm [158,159] has been used for parameter estimation of solar PV cells based on experimental *I–V* data. *RMSE* is the objective function. In this modified version, in order to enhance exploitation capability, crossover operator and merging operator are incorporated. The merging operator is based on logistic map function. The results on three different PV types, approve the outperformance of the proposed mutative scale parallel chaos optimisation algorithm over ABC [27], PS, SA, HS, GA and PSO.

In [160], hybrid of SA and Levenberg–Marquardt (LM) algorithm [161] has been used for parameter estimation of solar PV cells via experimental *I–V* data. Again, *RMSE* is the objective function. Single diode model for PV cells has been used. In LM, damping factor plays crucial role in convergence behaviour. In this work, optimal value of damping factor of LM is determined by SA. The results approve the outperformance of the proposed hybrid optimisation algorithm over GA, SA, PS, DE, PSO, HS, ABC [27] and Newton [110].

Other than the analysed applications of metaheuristics in solving parameter estimation problem of solar PV cells, there exist some other research works that have applied metaheuristics to this problem. In [47,162–168], GA, in [166,169–172], PSO, in [173], BFOA, in [166], DE and in [174], Chaotic PSO have been used for parameter estimation of solar PV cells.

In [175], a comparative analysis on the performance of different metaheuristics on parameter estimation of solar PV cells has been done. Double diode model has been used for PV cells. GA, PSO and two different DE variants including penalty-based DE and boundary-based DE have been used in comparisons. In boundary-based constraint handling strategy, if each decision variable exceeds its upper bound, it will be fixed at upper bound and if it goes below its lower bound, it will be fixed at lower bound. DE/best/1/bin has been used. The comparison has been done in terms of accuracy, consistency, convergence speed and number of control parameters. PV modules of different types, including multi-crystalline, mono-crystalline and thin-film have been used. Similar to most of research works, *RMSE* has been used as objective function. Synthetic data has been used for evaluating the performance of different metaheuristics. In terms of accuracy, penalty-based DE provides the best performance, followed by boundary-based DE, PSO and GA. Moreover, in terms of consistency and convergence speed, penalty-based DE outperform all other compared algorithms. In terms of the number of control parameters, penalty-based DE and boundary-based DE with two control parameters have the least number of control parameters while GA and PSO have four control parameters. In overall, this comparative analysis recommends using penalty-based DE for solving parameter estimation problem of solar PV cells.

In [176], the performance of a very diverse set of metaheuristic optimisation algorithms including hybrid ABC-DE, DE, ABC, SA, PSO, HS, bird mating optimisation (BMO) and Innovative global harmony search (IGHS) in estimating circuit model parameters of solar PV cells has been compared. The analysis show that in terms of the accuracy of estimation results, hybrid ABC-DE, DE, ABC and PSO outperform other used algorithms. Moreover, hybrid ABC-DE algorithm provides the fastest convergence speed among all compared metaheuristics (Table 3).

3.3. Hybrid analytical-metaheuristics for parameter estimation of PV cells

As mentioned before, the third category of solar PV cell circuit model parameter estimation approaches are hybrids of analytical and metaheuristic approaches, meaning that some parameters (commonly photocurrent and saturation current) are computed analytically and optimisation problem is formulated in a way to find optimal values of other parameters using metaheuristic optimisation algorithms. In this subsection, the application of hybrid analytical-metaheuristics approaches for parameter estimation of PV cells will be reviewed.

In [179], a hybrid analytical-metaheuristic approach has been used in order to estimate model parameters of PV cells with single diode model. I_{PV} and I_S are computed via analytical method and the remained three parameters are found by DE/best/1/bin, where 1 represents the number of mutation vectors and "bin" represents binomial crossover. The decision vector is as below.

$$X = [a, R_S, R_P] \tag{49}$$

Voltage and current at maximum power point which are available in datasheet, are used for parameter estimation. The objective function is the same with (48) and ranges of decision variables are as follows.

$R_S \in [0.1, 1]\Omega$, $R_P \in [100, 3000]\Omega$, $a \in [1, 2]$

Based on datasheet information, it computes circuit model parameters for different temperatures and irradiations. For validation, three different PV modules, i.e., multi-crystalline, mono-crystalline and thin-film have been tested. For verification, experimental *I–V* points have been used. Be noted that in this work, experimental *I–V* points have only been used for verification of the estimated parameters not extraction of the parameters.

In [60], another hybrid analytical-metaheuristic approach has been used in order to estimate model parameters of PV cells with single diode model. Diode's ideality factor, series and shunt resistance are computed by linearly decreasing inertia weight PSO. Only datasheet information has been used for parameter estimation. The objective function is formulated as Eqs. (50)–(53).

$$K_1 = \left|\frac{I_{SC}}{I_{SC,e}} - 1\right| \tag{50}$$

$$K_2 = \left|\frac{V_{OC}}{V_{OC,e}} - 1\right| \tag{51}$$

$$K_3 = \left|\frac{P_{mp}}{P_{mp,e}} - 1\right| \tag{52}$$

$$OF = |K_1 + K_2 + K_3| \tag{53}$$

where *OF* denotes objective function, I_{SC}, V_{OC} and P_{mp} are respectively estimated short circuit current, estimated open circuit voltage and estimated maximum power, $I_{SC,e}$, $V_{OC,e}$ and $P_{mp,e}$ are respectively datasheet values for short circuit current, open circuit voltage and maximum power

Ranges for decision variables are as follows. $R_S \in [0, 0.5]\Omega$, $R_P \in [50, 170]\Omega$, $a \in [1, 2]$. The results show that the difference between maximum power with estimated parameters and experimental maximum power is less than 0.02%. In this work, the procedure of computing photocurrent and saturation current has not been explained. The results have been obtained for different temperatures. Penalty function has been added to objective function in order to push the particles toward feasible regions of search space.

In [180], GA has been used in for estimating diode's ideality factor, series and shunt resistance in single and double diode model [181–183]. Experimental data have been used for parameter estimation. Mean absolute error metric, defined by (45), is the objective function and decision variables are bounded within the following ranges. $R_S \in [0.01, 1.2]\Omega$, $R_P \in [50, 1000]\Omega$, $a \in [1, 2]$. For single diode model, the decision vector is the same as (49) and for double diode model, the decision vector is as below.

$$X = [a_1, a_1, R_S, R_P] \tag{54}$$

Photocurrent and saturation currents of diodes are computed analytically. For validation, three different PV modules, i.e., multi-crystalline, mono-crystalline and thin-film have been tested. The results have been found for different temperatures and irradiations.

In [153], Photocurrent and diode's saturation current are computed by direct formulae, while hybrid of GA and interior point algorithm is used for estimating three remained parameters of single diode model. Only datasheet information has been used for parameter estimation. In GA, in order to enhance diversity, a

Table 3
Different metaheuristic-based parameter estimation strategies.

Ref.	Used data	Availability of used data	Used model	Objective function	Optimisation algorithm	Range of decision variables	Remarks
[1]	Experimental *I–V* data	Not available in datasheet	Single and double diode	Normalised value of *RMSE*	Artificial bee colony	$R_S \in [0, 0.5]\Omega$, $R_P \in [0, 100]\Omega$, $I_{PV} \in [0, 1]A$, $I_S \in [0, 1]\mu A$, $a \in [1, 2]$	The results approve the superiority of ABC algorithm over HS, PSO, GA and BFOA. in both in terms of accuracy and robustness.
[27]	Experimental *I–V* data	Not available in datasheet	Single and double diode	*RMSE*	A modified artificial bee colony [111]	$R_S \in [0, 0.5]\Omega$, $R_P \in [0, 100]\Omega$, $I_{PV} \in [0, 1]A$, $I_S \in [0, 1]\mu A$, $a \in [1, 2]$	The proposed modified ABC outperforms GA, SA, PS, HS and chaotic PSO. The results show that the difference between single diode and double diode models is only 0.79% that indicates the suitability of single diode model.
[117]	Datasheet information	Available in datasheet	Single diode model	*RMSE*	Scaling factor and crossover rate are controlled adaptively during the run.	$R_S \in [0.1, 2]\Omega$, $R_P \in [100, 5000]\Omega$, $I_{PV} \in [1, 8]A$, $I_S \in [1e-12, 1e-5]\mu A$, $a \in [1, 2]$	Model parameters have been separately extracted for seven different irradiation values. The findings approve the outperformance of the proposed adaptive DE over penalty-based DE [118] and an analytical approach. In DE, scaling factor and crossover rate are controlled adaptively during the run.
[118]	Synthetic data from two diode model	Not available in datasheet	Two diode model	*RMSE*	Penalty-based DE	$R_S \in [0, 1]\Omega$, $R_P \in [50, 1000]\Omega$, $I_{PV} \in [0, 7.6]A$, $I_{S1} \in [1e-12, 1e-5]\mu A$, $a_1 \in [0.5, 4], I_{S2} \in [1e-12, 1e-5]\mu A, a_2 \in [0.5, 4], I_{S2} \in [2, 7]I_{S1}$	The results on solar modules of different types indicate the outperformance of the proposed penalty-based PSO over GA, SA and PSO. The proposed penalty-based DE performs well in all terms of accuracy, consistency and convergence speed.
[119]	Both Synthetic and experimental data	Not available in datasheet	single diode model	*RMSE*	DE with adaptive strategy for scaling factor and crossover rate	$R_S \in [0, 2]\Omega$, $R_P \in [50, 5000]\Omega$, $I_{PV} \in [0, 5]A$, $I_S \in [1e-12, 1e-5]\mu A$, $a \in [0.5, 10]$ The upper range set for ideality factor of diode seems unusual.	The results testify the superiority of the proposed adaptive DE over PSO, GA, conventional DE, SA and an analytical approach. An important advantage of the proposed adaptive DE is that it does not require the tuning of any control parameter.
[120]	Experimental data	Not available in datasheet	Both single and double diode model	*RMSE*	An improved version of JADE [121]	$R_S \in [0, 0.5]\Omega$, $R_P \in [0, 100]\Omega$, $I_{PV} \in [0, 1]A$, $I_S \in [0, 1]\mu A$, $a \in [1, 2]$	The proposed modified JADE outperforms PSO, SA, ABC [27], HS, PS, Newton, JADE and some other DE variants.
[131]	Datasheet information	Available in datasheet	Double diode and three-diode model	$MAE = \frac{\sum_{i=1}^{N}(I_{i,exp} - I_{i,est})}{N}$	Linearly decreasing inertia weight PSO	Has not been mentioned.	The findings show that the three diode model provides more accuracy than two diode model. The proposed PSO has outperformed DE.
[132,133]	Experimental *I–V* data	Not available in datasheet	Single diodemodel	$OF = \sum_{i=1}^{N} abs(I_{i,exp} - I_{i,est})$	Pattern search	Not mentioned	Pattern search outperforms GA, Newton method [110,136].
[137]	Experimental *I–V* data	Not available in datasheet	Both single and double diode model	*RMSE*	BBO with chaotic-based mutation strategy	$R_S \in [0, 0.5]\Omega$, $R_P \in [0, 100]\Omega$, $I_{PV} \in [0, 1]A$, $I_S \in [0, 1]\mu A$, $a \in [1, 2]$	The proposed mutation-integrated BBO provides desirable accuracy and convergence speed. It outperforms conventional BBO, PSO, GA, DE, PS, ABC, SA, HS and chaotic PSO.
[144]	26 pairs of experimental *I–V* data from [110]	Not available in datasheet	Single and double diode	*RMSE*	Innovative global harmony search (IGHS)	$R_S \in [0, 0.5]\Omega$, $R_P \in [0, 100]\Omega$, $I_{PV} \in [0, 1]A$, $I_S \in [0, 1]\mu A$, $a \in [1, 2]$	Innovative global harmony search (IGHS) outperforms conventional HS, SA and PS.
[145]	Experimental *I–V* data	Not available in datasheet	Single and double diode	$OF = \sum_{i=1}^{N} abs(I_{i,exp} - I_{i,est})$	SA	Not mentioned.	SA outperforms [136,110]
[148]	Experimental *I–V* data			*RMSE*		$R_S \in [0, 0.5]\Omega$, $R_P \in [0, 100]\Omega$, $I_{PV} \in [0, 1]A$, $I_S \in [0, 1]\mu A$, $a \in [1, 2]$	BMO outperforms PS, SA, HS, ABC, PSO, GA and IGHS [144].

		Not available in datasheet	Single and double diode		Bird mating optimisation (BMO)		
[149]	Experimental *I–V* data	Not available in datasheet	Single and double diode	*RMSE*	Flower pollination algorithm	$I_{PV} \in [0,2]\text{A},\ I_S \in [0,1]\mu\text{A}$	Flower pollination algorithm outperforms Newton method [110], BFOA, DE, HS, ABC, PS, hybrid GA-interior point [153], parallel chaos optimisation [154] and cuckoo search optimisation (CSO).
[155]	Experimental *I–V* data	Not available in datasheet	Single and double diode	*RMSE*	A modified TLBO	$R_S \in [0,0.5]\Omega,\ R_P \in [0,100]\Omega,\ I_{PV} \in [0,1]\text{A},\ I_S \in [0,1]\mu\text{A},\ a \in [1,2]$	The proposed modified TLBO outperforms conventional TLBO, ABC [27], innovative global harmony search [144], PS and SA. However, it introduces a control parameter that must be tuned by user.
[154]	Experimental *I–V* data	Not available in datasheet	Single and double diode	*RMSE*	A modified version of chaos optimisation algorithm [158,159]	Not mentioned.	The results approve the outperformance of the proposed mutative scale parallel chaos optimisation algorithm over ABC [27], PS, SA, HS, GA and PSO.
[160]	Experimental *I–V* data	Not available in datasheet	Single diode	*RMSE*	SA has been hybridised with Levenberg–Marquardt (LM) algorithm.	Not mentioned.	The results approve the superiority of the proposed hybrid algorithm over GA, SA, PS, DE, PSO, HS, ABC [27] and Newton [110].
[177,178]	Experimental *I–V* data	Not available in datasheet	Double diode	$OF = \frac{dI}{dV}(\text{mpp}) + \frac{I_{mp}}{V_{mp}}$ (48)	Artificial immune system (AIS)	Not mentioned.	The findings indicate the outperformance of AIS over GA and PSO.

disruptive selection method, a dynamically controlled mutation rate strategy and a random offspring generation strategy have been incorporated. For KC200GT, ranges of decision variables are $R_S \in [0.001, 1]\Omega$, $R_P \in [50, 1100]\Omega$, $a \in [1, 2]$, for ST40, ranges of decision variables are $R_S \in [0.001, 1]\Omega$, $R_P \in [50, 550]\Omega$, $a \in [1, 2]$, and for E20/33, ranges of decision variables are $R_S \in [0.001, 2]\Omega$, $R_P \in [50, 1500]\Omega$, $a \in [1, 2]$.

In this work, assuming that maximum power at standard test condition (STC) and normal operating cell temperature (NOCT) condition are available, the values of ideality factor, series resistance and shunt resistance are found in a way that the maximum output power at standard and normal conditions get as close as possible to those values. The objective function is formulated as below.

$$J_1 = \left\| \frac{V_{STC} - V_{mpp,STC}}{V_{mpp,STC}}, \frac{I_{STC} - I_{mpp,STC}}{I_{mpp,STC}}, \frac{P_{STC} - P_{mpp,STC}}{P_{mpp,STC}} \right\| \tag{55}$$

$$J_2 = \left\| \frac{V_{NOCT} - V_{mpp,NOCT}}{V_{mpp,NOCT}}, \frac{I_{NOCT} - I_{mpp,NOCT}}{I_{mpp,NOCT}}, \frac{P_{NOCT} - P_{mpp,NOCT}}{P_{mpp,NOCT}} \right\| \tag{56}$$

$$J = W_1 J_1 + W_2 J_2 \tag{57}$$

where V_{STC}, I_{STC} and P_{STC} are voltage, current and power of PV cell at standard test conditions, V_{NOCT}, I_{NOCT} and P_{NOCT} are voltage, current and power of PV cell at normal conditions. $V_{mpp,STC}$, $I_{mpp,STC}$ and $P_{mpp,STC}$ are datasheet values for voltage at maximum power, current at maximum power and maximum power at standard test conditions. $V_{mpp,NOCT}$, $I_{mpp,NOCT}$ and $P_{mpp,NOCT}$ are datasheet values for voltage at maximum power, current at maximum power and maximum power at normal conditions. In (57), J represents objective function and weight factors W_1 and W_2 have been set as 0.5. Three PV modules including KC200GT, ST40 and E20/33 have been used. The results testify the outperformance of the proposed GA-IP method over PSO.

In [184], hybrid of analytical approach and pattern search has been used for estimating parameters of single diode model via datasheet information. Photocurrent and diode's saturation current are found analytically and other parameters are determined by pattern search.

$$OF = \left(I_{mp} - I_{mp,est}\right)^2 + \frac{dI}{dV}(\text{mpp}) + \frac{I_{mp}}{V_{mp}} \tag{58}$$

In this work, the following constraints are specified for series and shunt resistances.

$$0 \le R_S \le \frac{V_{OC} - V_{mpp}}{I_{mpp}} \tag{59}$$

$$0 \le R_P \le \frac{V_{mpp}}{I_{SC} - I_{mpp}} \tag{60}$$

In [61], Photocurrent and diode's saturation current are found analytically and BFOA is used to find other circuit model parameters of PV cells using datasheet information [185–187]. Objective function is the same as (48). For validation, three different PV modules, i.e., multi-crystalline, mono-crystalline and thin-film have been tested. The results testify that BFOA outperforms GA and artificial immune system (AIS) optimisation algorithm. It provides high accuracy and robustness, however suffers from slow convergence speed (Table 4).

3.4. Discussion on applications of pure metaheuristics and hybrid analytical-metaheuristics in PV cell parameter estimation problem

Now, in this sub-section, based on the materials of Sections 3.2 and 3.3, diverse applications of metaheuristics and hybrid analytical-metaheuristics to parameter estimation of PV cells, are discussed from different perspectives.

From the perspective of the data used for parameter estimation, the existing research works can be classified into three categories; in most of them, experimental *I–V* data are used [1,27,120,132,133,137,144,148,149,154,155,160,177,178,180], however, due to measurement noise, such data is noisy and the noise affects the accuracy of estimated parameters. Datasheet information is the other type of data used for parameter estimation of PV cells [60,61,117,131,153,179,184]. In few cases, for evaluating the performance of the parameter estimation strategies, synthetic data is used, that is, *I–V* data is generated based on known values of model parameters [118].

From the viewpoint of the availability of used data, the research works can be classified into two categories; those whose data are available in datasheet [60,61,117,131,153,179,184] and those which are not so [1,27,120,132,133,137,144,148,149,154,155,160,177,178,180].

From the perspective of the PV cell model, single diode model, due to appropriate trade-off between accuracy and simplicity, is the most commonly used model [1,27,60,61,117,119,120,132,133,137,144,148,149,153–155,160,179,180,184]. In few cases, parameter estimation has been done for double diode [1,27,118,120,131,144,148,149,154,155,177–180] and three diode models [131].

From the perspective of objective function, in most of cases, *RMSE* is the objective function [1,27,117,118,120,137,148,149,154,155,160]. In few cases, the derivative of power with respect to voltage at maximum power point is the objective function [177,178]. The other objective functions used in literature are mean absolute error (MAE) in [131] and sum of absolute errors in [132,133,145].

From the perspective of the used metaheuristic optimisation algorithm, GA is the most commonly used algorithm and PSO is the second most common metaheuristic for solving PV cell parameter estimation problem. GA [47,162–168,180], PSO [60,131,166,169–172], DE [118–121,166,179], PS [132,133,184], ABC [1,27], BFOA [61,173], AIS [177,178], BBO [137], IGHS [144], SA [145], BMO [148], Flower pollination algorithm [149], TLBO [155], Chaos optimisation algorithm [154], Hybrid of SA and Levenberg–Marquardt (LM) algorithm [160], Hybrid GA-interior point [153] and chaotic PSO [174] are the metaheuristics that have already been applied to PV cell parameter estimation problem.

From the perspective of ranges specified for circuit model parameters, the most commonly used ranges are $R_S \in [0, 0.5]\Omega$, $R_P \in [0, 100]\Omega$, $I_{PV} \in [0, 1]$A, $I_S \in [0, 1]\mu$A, $a \in [1, 2]$ [1,27,120,137,144,148,155].

4. Overall review on parameter estimation of PV cells and some directions for future research

After reviewing the existing research works on parameter estimation of solar PV cells, the following points must be considered.

- Experimental data, due to measurement noise result in inaccuracy of estimated model parameters. Moreover, during the measurement of *I–V* data, temperature and irradiation may change that affects the measured *I–V* data and thereby affects the accuracy of parameter estimation. Appropriate consideration of noise in formulation of optimisation problem and finding efficient strategies to handle the resultant noisy optimisation problem is recommended for future research.

Table 4
Different hybrid analytical-metaheuristics parameter estimation strategies.

Ref.	Used data	Availability of used data	Used model	Objective function	Used optimisation algorithm	Range of decision variables	Remarks
[179]	Voltage and current at maximum power point	Available in datasheet	Single diode model	$OF = \frac{dI}{dV}(\mathrm{mpp}) + \frac{I_{mp}}{V_{mp}}$	DE/best/1/bin	$R_S \in [0.1, 1]\Omega$, $R_P \in [100, 3000]\Omega$, $a \in [1, 2]$	I_{PV} and I_S are computed via analytical method. For validation, three different PV modules, i.e., multi-crystalline, mono-crystalline and thin-film have been tested. For verification, experimental I–V points have been used.
[60]	Datasheet information	Available in datasheet	Single diode model	Eqs. (50)–(53)	Linearly decreasing inertia weight PSO	$R_S \in [0, 0.5]\Omega$, $R_P \in [50, 170]\Omega$, $a \in [1, 2]$	The results show that the difference between maximum power with estimated parameters and experimental maximum power is less than 0.02%.
[180]	Experimental data of different temperatures and irradiation	Not available in datasheet	Single and double diode model	Mean absolute error metric, defined by (45)	GA	$R_S \in [0.01, 1.2]\Omega$, $R_P \in [50, 1000]\Omega$, $a \in [1, 2]$	Photocurrent and saturation currents of diodes are computed analytically. The results have been found for different temperatures and irradiations.
[153]	Datasheet information	Available in datasheet	Single diode model	Eqs. (55)–(57)	Hybrid of GA and interior point	For KC200GT, $R_S \in [0.001, 1]\Omega$, $R_P \in [50, 1100]\Omega$, $a \in [1, 2]$, for ST40, $R_S \in [0.001, 1]\Omega$, $R_P \in [50, 550]\Omega$, $a \in [1, 2]$ and for E20/33 $R_S \in [0.001, 2]\Omega$, $R_P \in [50, 1500]\Omega$, $a \in [1, 2]$	The results testify the outperformance of the proposed GA-IP method over PSO.
[184]	Datasheet info	Available in datasheet	Single diodemodel	Defined by (58)	Pattern search	Inequalities (59) and (60)	Crystalline PV array has been used. Photocurrent and diode's saturation current are found analytically.
[61]	Datasheet info	Available in datasheet	Single diodemodel	Defined by (48)	BFOA	Not mentioned.	BFOA outperforms GA and artificial immune system optimisation algorithm. It provides high accuracy and robustness, however suffers from slow convergence speed.

- Since computational time of parameter estimation strategies, especially in certain applications is crucial, the research effort must be put to reduce their computational time.
- Although, some metaheuristic optimisation algorithms have already been applied to solve PV cell parameter estimation problem, using other metaheuristics such as imperialistic competitive algorithm (ICA), brainstorm optimisation algorithm (BSOA), bat swarm optimisation (BSO) algorithm, firefly swarm optimisation (FSO) algorithm, cuckoo search optimisation (CSO) algorithm, evolutionary programming (EP), invasive weed optimisation (IWO), grey wolf optimisation (GWO) algorithm, seeker optimisation algorithm (SOA), evolution strategy (ES), krill herd optimisation (KHO) to PV cell parameter estimation problem, in the hope of achieving better results than existing parameter estimation strategies is highly recommended.
- Control parameters of metaheuristic optimisation algorithms significantly affect their computational behaviour. The suitable values of control parameters are different from problem to problem. For each optimisation problem, the suitable values of control parameters must be determined. However, in none of the existing research works, the control parameters of metaheuristics have been tuned.
- A detailed comparison between pure metaheuristic approaches and hybrid analytical-metaheuristic approaches in terms of accuracy, robustness, convergence speed and computational time is recommended.
- Comparing the performance of a very diverse set of metaheuristics on PV cell parameter estimation problem in terms of accuracy, robustness and convergence speed and identifying the most appropriate metaheuristic(s) for solving this problem will be an interesting and useful research thread for future.
- In cases where experimental *I–V* data are used for parameter estimation of solar PV cells, using data sets with larger number of *I–V* data points can lead to results of higher accuracy, although computational time increases.
- The appropriate objective function for PV cell parameter estimation problem, depends on the application. For example, for maximum power point tracking applications, some of errors between estimated maximum power and measured maximum power seems to be an appropriate objective function. Therefore, choosing objective function based on the application of the PV cell model is recommended.

5. Conclusions

PV cell model parameter estimation is a hot research topic in renewable energy. In this paper, different circuit models of PV cells have been described and the existing research works on PV cell model parameter estimation problem have been categorised into three categories and the research works of those categories have been reviewed. Based on the conducted review, some proposals for future research have been provided. The findings of this review indicate that although a great deal of research effort has been put for solving parameter estimation problem in PV cells, there is still room for improvement. The author strongly believes that this paper would be helpful for researchers and engineers in the related field.

References

[1] Oliva D, Cuevas E, Pajares G. Parameter identification of solar cells using artificial bee colony optimization. Energy 2014;72:93–102.
[2] Energy at the crossroads; 2015. ⟨http://home.cc.umanitoba.ca/~vsmil/pdf_pubs/oecd.pdf⟩.
[3] Where-is-solar-power-used-the-most; 2015. ⟨http://energyinformative.org⟩.
[4] Bai J, Liu S, Hao Y, Zhang Z, Jiang M, Zhang Y. Development of a new compound method to extract the five parameters of PV modules. Energy Convers Manag 2014;79:294–303.
[5] Shafiee S, Topal E. When will fossil fuel reserves be diminished? Energy Policy 2009;37:181–9.
[6] Apergis N, Payne JE. Renewable energy, output, CO 2 emissions, and fossil fuel prices in Central America: evidence from a nonlinear panel smooth transition vector error correction model. Energy Econ 2014;42:226–32.
[7] Shivalkar R, Jadhav H, Deo P. Feasibility study for the net metering implementation in rooftop solar PV installations across reliance energy consumers. In: proceedings of international conference on circuit, power and computing technologies (ICCPCT 2015). IEEE; 2015. p. 1–6.
[8] Wang Y, Zhou S, Huo H. Cost and CO_2 reductions of solar photovoltaic power generation in China: perspectives for 2020. Renew Sustain Energy Rev 2014;39:370–80.
[9] Sundareswaran K, Sankar P, Nayak P, Simon SP, Palani S. Enhanced energy output from a PV system under partial shaded conditions through artificial bee colony. Sustain Energy IEEE Trans 2015;6:198–209.
[10] The Solar Singularity is Nigh; 2015. ⟨http://www.greentechmedia.com/articles⟩.
[11] Dusonchet L, Telaretti E. Economic analysis of different supporting policies for the production of electrical energy by solar photovoltaics in western European Union countries. Energy Policy 2010;38:3297–308.
[12] Solangi K, Islam M, Saidur R, Rahim N, Fayaz H. A review on global solar energy policy. Renew Sustain Energy Rev 2011;15:2149–63.
[13] Branker K, Pearce JM. Financial return for government support of large-scale thin-film solar photovoltaic manufacturing in Canada. Energy Policy 2010;38:4291–303.
[14] Campoccia A, Dusonchet L, Telaretti E, Zizzo G. Comparative analysis of different supporting measures for the production of electrical energy by solar PV and Wind systems: four representative European cases. Sol Energy 2009;83:287–97.
[15] Timilsina GR, Kurdgelashvili L, Narbel PA. Solar energy: markets, economics and policies. Renew Sustain Energy Rev 2012;16:449–65.
[16] Karaveli AB, Soytas U, Akinoglu BG. Comparison of large scale solar PV (photovoltaic) and nuclear power plant investments in an emerging market. Energy 2015;84:656–65.
[17] Clò S, D'Adamo G. The dark side of the sun: how solar power production affects the market value of solar and gas sources. Energy Econ 2015;49:523–30.
[18] Köberle AC, Gernaat DE, van Vuuren DP. Assessing current and future techno-economic potential of concentrated solar power and photovoltaic electricity generation. Energy 2015.
[19] Reca J, Torrente C, López-Luque R, Martínez J. Feasibility analysis of a standalone direct pumping photovoltaic system for irrigation in Mediterranean greenhouses. Renew Energy 2016;85:1143–54.
[20] Kamjoo A, Maheri A, Dizqah AM, Putrus GA. Multi-objective design under uncertainties of hybrid renewable energy system using NSGA-II and chance constrained programming. Int J Electr Power Energy Syst 2016;74:187–94.
[21] Nanou SI, Papakonstantinou AG, Papathanassiou SA. A generic model of two-stage grid-connected PV systems with primary frequency response and inertia emulation. Electr Power Syst Res 2015;127:186–96.
[22] Moura AP, Lopes JAP, de Moura AAF, Sumaili J, Moreira CL. IMICV fault analysis method with multiple PV grid-connected inverters for distribution systems. Electr Power Syst Res 2015;119:119–25.
[23] Arulkumar K, Vijayakumar D, Palanisamy K. Modeling and control strategy of three phase neutral point clamped multilevel PV inverter connected to the grid. J Build Eng 2015;3:195–202.
[24] Villalva MG, Gazoli JR. Comprehensive approach to modeling and simulation of photovoltaic arrays. Power Electron IEEE Trans 2009;24:1198–208.
[25] Chin VJ, Salam Z, Ishaque K. Cell modelling and model parameters estimation techniques for photovoltaic simulator application: a review. Appl Energy 2015;154:500–19.
[26] Venugopalan R, Krishnakumar N, Sudhakarbabu T, Sangeetha K, Rajasekar N. Modified Particle Swarm Optimization technique based Maximum Power Point Tracking for uniform and under partial shading condition. Appl Soft Comput 2015.
[27] Askarzadeh A, Rezazadeh A. Artificial bee swarm optimization algorithm for parameters identification of solar cell models. Appl Energy 2013;102:943–9.
[28] Farivar G, Asaei B. Photovoltaic module single diode model parameters extraction based on manufacturer datasheet parameters. In: proceedings of IEEE international conference on Power and energy (PECon 2010). IEEE; 2010. p. 929–34.
[29] Kim W, Choi W. A novel parameter extraction method for the one-diode solar cell model. Sol Energy 2010;84:1008–19.
[30] Caracciolo F, Dallago E, Finarelli DG, Liberale A, Merhej P. Single-variable optimization method for evaluating solar cell and solar module parameters. Photovolt IEEE J 2012;2:173–80.
[31] Hansen CW, Luketa-Hanlin A, Stein JS. Sensitivity of single diode models for photovoltaic modules to method used for parameter estimation; 2013.
[32] Zaharatos BR, Campanelli M, Tenorio L. On the estimability of the PV single-diode model parameters. Stat Anal Data Min: ASA Data Sci J 2015.
[33] Hansen C. Parameter Estimation for Single Diode Models of Photovoltaic Modules, Sandia National Laboratories, Albuquerque, NM, Forthcoming; 2015.

[34] Balzani M, Reatti A. Neural network based model of a PV array for the optimum performance of PV system, in: research in microelectronics and electronics (Ph.D.), 2005, IEEE; 2005. p. 123–26.

[35] Almonacid F, Rus C, Hontoria L, Muñoz F. Characterisation of PV CIS module by artificial neural networks. A comparative study with other methods. Renew Energy 2010;35:973–80.

[36] Almonacid F, Rus C, Hontoria L, Fuentes M, Nofuentes G. Characterisation of Si-crystalline PV modules by artificial neural networks. Renew Energy 2009;34:941–9.

[37] Piliougine M, Elizondo D, Mora-López L, Sidrach-de-Cardona M. Modelling photovoltaic modules with neural networks using angle of incidence and clearness index. Prog Photovolt: Res App 2015;23:513–23.

[38] Fathabadi H. Novel neural-analytical method for determining silicon/plastic solar cells and modules characteristics. Energy Convers Manag 2013;76:253–9.

[39] Chegaar M, Ouennoughi Z, Hoffmann A. A new method for evaluating illuminated solar cell parameters. Solid-State Electron 2001;45:293–6.

[40] Kajihara A, Harakawa T. Model of photovoltaic cell circuits under partial shading. In: proceedings of IEEE international conference on industrial technology, 2005 (ICIT 2005). IEEE; 2005. p. 866–70.

[41] Dash SK, Raj RA, Nema S, Nema R. Development of photovoltaic (PV) cell/module/array and non-uniform irradiance effect based on two-diode model by using PSPICE simulator, in: proceedings of international conference on nascent technologies in the engineering field (ICNTE 2015). IEEE; 2015. p. 1–6.

[42] Vergura S. Scalable model of PV cell in variable environment condition based on the manufacturer datasheet for circuit simulation. In: proceedings of IEEE 15th international conference on environment and electrical engineering (EEEIC 2015). IEEE; 2015. p. 1481–85.

[43] Kadri R, Andrei H, Gaubert J-P, Ivanovici T, Champenois G, Andrei P. Modeling of the photovoltaic cell circuit parameters for optimum connection model and real-time emulator with partial shadow conditions. Energy 2012;42:57–67.

[44] Andrei H, Cepisca C, Grigorescu S, Ivanovici T, Andrei P. ModelLing of the PV panels circuit parameters using the 4-terminals equations and Brune's conditions. Sci Bull Electr Eng Fac 2010;10:2010.

[45] Salmi T, Bouzguenda M, Gastli A, Masmoudi A. Matlab/simulink based modeling of photovoltaic cell. Int J Renew Energy Res 2012;2:213–8.

[46] Das N, Wongsodihardjo H, Islam S. Modeling of multi-junction photovoltaic cell using MATLAB/Simulink to improve the conversion efficiency. Renew Energy 2015;74:917–24.

[47] Awadallah MA, Venkatesh B. Estimation of PV module parameters from datasheet information using optimization techniques. In: proceedings of IEEE international conference on industrial technology (ICIT 2015). IEEE; 2015. p. 2777–82.

[48] Sandrolini L, Artioli M, Reggiani U. Numerical method for the extraction of photovoltaic module double-diode model parameters through cluster analysis. Appl Energy 2010;87:442–51.

[49] Garrido-Alzar C. Algorithm for extraction of solar cell parameters from I–V curve using double exponential model. Renew Energy 1997;10:125–8.

[50] Liu G, Nguang SK, Partridge A. A general modeling method for I–V characteristics of geometrically and electrically configured photovoltaic arrays. Energy Convers Manag 2011;52:3439–45.

[51] Ortiz-Conde A, Sánchez FJG, Muci J. New method to extract the model parameters of solar cells from the explicit analytic solutions of their illuminated I–V characteristics. Sol Energy Mater Sol Cells 2006;90:352–61.

[52] Saleem H, Karmalkar S. An analytical method to extract the physical parameters of a solar cell from four points on the illuminated curve. Electron Device Lett IEEE 2009;30:349–52.

[53] Chan D, Phillips J, Phang J. A comparative study of extraction methods for solar cell model parameters. Solid-State Electron 1986;29:329–37.

[54] Jain A, Kapoor A. Exact analytical solutions of the parameters of real solar cells using Lambert W-function. Sol Energy Mater Sol Cells 2004;81:269–77.

[55] Romero B, del Pozo G, Arredondo B. Exact analytical solution of a two diode circuit model for organic solar cells showing S-shape using Lambert W-functions. Sol Energy 2012;86:3026–9.

[56] Ahmad M, Talukder A-A, Tanni MA. Estimation of important parameters of photovoltaic modules from manufacturer's datasheet. In: proceedings of international conference on informatics, electronics & vision (ICIEV 2012). IEEE; 2012. p. 571–76.

[57] Di Piazza MC, Luna M, Vitale G. Dynamic PV model parameter identification by least-squares regression. Photovolt IEEE J 2013;3:799–806.

[58] Park H, Kim H. PV cell modeling on single-diode equivalent circuit, In: proceedings of the 39th annual conference of the IEEE industrial electronics society (IECON 2013). IEEE; 2013. p. 1845–49.

[59] Kumar G, Panchal AK. A non-iterative technique for determination of solar cell parameters from the light generated IV characteristic. J Appl Phys 2013;114:084904.

[60] Soon JJ, Low K-S. Photovoltaic model identification using particle swarm optimization with inverse barrier constraint. Power Electron IEEE Trans 2012;27:3975–83.

[61] Rajasekar N, Kumar NK, Venugopalan R. Bacterial foraging algorithm based solar PV parameter estimation. Sol Energy 2013;97:255–65.

[62] Ciulla G, Brano VL, Di Dio V, Cipriani G. A comparison of different one-diode models for the representation of I–V characteristic of a PV cell. Renew Sustain Energy Rev 2014;32:684–96.

[63] Lim LHI, Ye Z, Ye J, Yang D, Du H. A linear method to extract diode model parameters of solar panels from a single I–V curve. Renew Energy 2015;76:135–42.

[64] Gow J, Manning C. Development of a model for photovoltaic arrays suitable for use in simulation studies of solar energy conversion systems; 1996.

[65] Chowdhury S, Taylor G, Chowdhury S, Saha A, Song Y. Modelling, simulation and performance analysis of a PV array in an embedded environment. In: proceedings of the 42nd international universities power engineering conference, 2007 (UPEC 2007). IEEE; 2007. p. 781–85.

[66] Gupta S, Tiwari H, Fozdar M, Chandna V. Development of a two diode model for photovoltaic modules suitable for use in simulation studies. In: proceedings of Asia-Pacific power and energy engineering conference (APPEEC 2012). IEEE; 2012. p. 1–4.

[67] Suskis P, Galkin I. Enhanced photovoltaic panel model for MATLAB-simulink environment considering solar cell junction capacitance, in: proceedings of the 39th annual conference of the IEEE industrial electronics society (IECON 2013). IEEE; 2013. p. 1613–18.

[68] Nishioka K, Sakitani N, Uraoka Y, Fuyuki T. Analysis of multicrystalline silicon solar cells by modified 3-diode equivalent circuit model taking leakage current through periphery into consideration. Sol Energy Mater Sol Cells 2007;91:1222–7.

[69] Kurobe K-i, Matsunami H. New two-diode model for detailed analysis of multicrystalline silicon solar cells. Jpn J Appl Phys 2005;44:8314.

[70] Mazhari B. An improved solar cell circuit model for organic solar cells. Sol Energy Mater Sol Cells 2006;90:1021–33.

[71] Lumb MP, Bailey CG, Adams JG, Hillier G, Tuminello F, Elarde VC, Walters R. Analytical drift-diffusion modeling of GaAs solar cells incorporating a back mirror. In: proceedings of IEEE 39th photovoltaic specialists conference (PVSC 2013). IEEE; 2013. p. 1063–68.

[72] Soon JJ, Low K-S, Goh ST. Multi-dimension diode photovoltaic (PV) model for different PV cell technologies. In: proceedings of IEEE 23rd international symposium on industrial electronics (ISIE 2014). IEEE; 2014. p. 2496–501.

[73] Ulapane NN, Dhanapala CH, Wickramasinghe SM, Abeyratne SG, Rathnayake N, Binduhewa PJ. Extraction of parameters for simulating photovoltaic panels. In: proceedings of the 6th IEEE international conference on industrial and information systems (ICIIS 2011). IEEE; 2011. p. 539–44.

[74] Bellini A, Bifaretti S, Iacovone V, Cornaro C. Simplified model of a photovoltaic module. In: Applied Electronics, 2009 (AE 2009). IEEE; 2009. p. 47–51.

[75] Walker G. Evaluating MPPT converter topologies using a MATLAB PV model. J Electr Electron Eng 2001;21:49–56.

[76] Kou Q, Klein S, Beckman W. A method for estimating the long-term performance of direct-coupled PV pumping systems. Sol Energy 1998;64:33–40.

[77] Chenni R, Makhlouf M, Kerbache T, Bouzid A. A detailed modeling method for photovoltaic cells. Energy 2007;32:1724–30.

[78] Walker GR. Evaluating MPPT converter topologies using a MATLAB PV model. AUPEC 2000: Innov Secure Power 2000;1:138–43.

[79] Xiao W, Dunford WG, Capel A, A novel modeling method for photovoltaic cells. In: proceedings of IEEE 35th annual power electronics specialists conference, 2004 (PESC 04). IEEE, 2004, p. 1950–56.

[80] Ding K, Bian X, Liu H, Peng T. A MATLAB-simulink-based PV module model and its application under conditions of nonuniform irradiance. Energy Convers IEEE Trans 2012;27:864–72.

[81] Shongwe S, Hanif M. Comparative analysis of different single-diode PV modeling methods. Photovolt IEEE J 2015;5:938–46.

[82] Chouder A, Silvestre S, Sadaoui N, Rahmani L. Modeling and simulation of a grid connected PV system based on the evaluation of main PV module parameters. Simul Model Pract Theory 2012;20:46–58.

[83] Arab AH, Chenlo F, Benghanem M. Loss-of-load probability of photovoltaic water pumping systems. Solar Energy 2004;76:713–23.

[84] Bashahu M, Nkundabakura P. Review and tests of methods for the determination of the solar cell junction ideality factors. Sol Energy 2007;81:856–63.

[85] Ortiz-Conde A, García-Sánchez FJ, Muci J, Sucre-González A. A review of diode and solar cell equivalent circuit model lumped parameter extraction procedures. Facta Univ Ser: Electron Energ 2014;27:57–102.

[86] Cotfas D, Cotfas P, Kaplanis S. Methods to determine the dc parameters of solar cells: a critical review. Renew Sustain Energy Rev 2013;28:588–96.

[87] Li Y, Huang W, Huang H, Hewitt C, Chen Y, Fang G, Carroll DL. Evaluation of methods to extract parameters from current–voltage characteristics of solar cells. Sol Energy 2013;90:51–7.

[88] Mares O, Paulescu M, Badescu V. A simple but accurate procedure for solving the five-parameter model. Energy Convers Manag 2015;105:139–48.

[89] De Blas M, Torres J, Prieto E, Garcıa A. Selecting a suitable model for characterizing photovoltaic devices. Renew energy 2002;25:371–80.

[90] Brano VL, Orioli A, Ciulla G, Di Gangi A. An improved five-parameter model for photovoltaic modules. Sol Energy Mater Sol Cells 2010;94:1358–70.

[91] Orioli A, Di Gangi A. A procedure to calculate the five-parameter model of crystalline silicon photovoltaic modules on the basis of the tabular performance data. Appl Energy 2013;102:1160–77.

[92] Sera D, Teodorescu R, Rodriguez P. PV panel model based on datasheet values. In: proceedings of IEEE international symposium on industrial electronics, 2007 (ISIE 2007). IEEE; 2007. p. 2392–96.

[93] Adamo F, Attivissimo F, Di Nisio A, Lanzolla A, Spadavecchia M. Parameters estimation for a model of photovoltaic panels. In: XIX IMEKO world congress fundamental applied metrology. Lisbon, Portugal; September, 2009. p. 6–11.

[94] Peng L, Sun Y, Meng Z. An improved model and parameters extraction for photovoltaic cells using only three state points at standard test condition. J Power Sources 2014;248:621–31.
[95] De Soto W, Klein S, Beckman W. Improvement and validation of a model for photovoltaic array performance. Sol energy 2006;80:78–88.
[96] Elbaset AA, Ali H, Abd-El Sattar M. Novel seven-parameter model for photovoltaic modules. Sol Energy Mater Sol Cells 2014;130:442–55.
[97] Belhaouas A, Cheikh A, Larbes C. Suitable Matlab-Simulink simulator for PV system based on a two-diode model under shading conditions. In: proceedings of the 3rd international conference on systems and control (ICSC 2013). IEEE, 2013, p. 72–6.
[98] Ahmed J, Salam Z. A Maximum Power Point Tracking (MPPT) for PV system using Cuckoo Search with partial shading capability. Appl Energy 2014;119:118–30.
[99] Ishaque K, Salam Z. A comprehensive MATLAB Simulink PV system simulator with partial shading capability based on two-diode model. Sol Energy 2011;85:2217–27.
[100] Ishaque K, Salam Z, Taheri H. Modeling and simulation of photovoltaic (PV) system during partial shading based on a two-diode model. Simul Model Pract Theory 2011;19:1613–26.
[101] Rezaee Jordehi A, Jasni J, Abd Wahab N, Kadir MZ, Javadi MS. Enhanced leader PSO (ELPSO): a new algorithm for allocating distributed TCSC's in power systems. Int J Electr Power Energy Syst 2015;64:771–84.
[102] Jordehi AR. Optimal setting of TCSC's in power systems using teaching-learning-based optimisation algorithm. Neural Comput Appl 2014.
[103] Jordehi AR. Optimisation of electric distribution systems: a review. Renew Sustaina Energy Rev 2015.
[104] Jordehi AR. Particle swarm optimisation (PSO) for allocation of FACTS devices in electric transmission systems: a review. Renew Sustain Energy Rev 2015;52:1260–7.
[105] Nesmachnow S. An overview of metaheuristics: accurate and efficient methods for optimisation. Int J Metaheuristics 2014;3:320–47.
[106] Gharravi HG, Farham MS. Applying metaheuristic approaches on the single facility location problem with polygonal barriers. Int J Metaheuristics 2014;3:348–70.
[107] Sambariya DK, Prasad R. Robust tuning of power system stabilizer for small signal stability enhancement using metaheuristic bat algorithm. Int J Electr Power Energy Syst 2014;61:229–38.
[108] Fidanova S, Marinov P, Paparzycki M. Multi-objective ACO algorithm for WSN layout: performance according to number of ants. Int J Metaheuristics 2014;3:149–61.
[109] Karaboga D, Basturk B. A powerful and efficient algorithm for numerical function optimization: artificial bee colony (ABC) algorithm. J Glob Optim 2007;39:459–71.
[110] Easwarakhanthan T, Bottin J, Bouhouch I, Boutrit C. Nonlinear minimization algorithm for determining the solar cell parameters with microcomputers. Int J Sol Energy 1986;4:1–12.
[111] Askarzadeh A, Rezazadeh A. A new artificial bee swarm algorithm for optimization of proton exchange membrane fuel cell model parameters. J Zhejiang Univ Sci C 2011;12:638–46.
[112] Jun-hua L, Ming L. An analysis on convergence and convergence rate estimate of elitist genetic algorithms in noisy environments. Optik - Int J Light Electron Opt 2013;124:6780–5.
[113] Pan H, Wang L, Liu B. Particle swarm optimization for function optimization in noisy environment. Appl Math Comput 2006;181:908–19.
[114] Attivissimo F, Nisio AD, Savino M, Spadavecchia M. Uncertainty analysis in photovoltaic cell parameter estimation. Instrum Meas IEEE Trans 2012;61:1334–42.
[115] Storn R, Price K. Differential evolution – a simple and efficient heuristic for global optimization over continuous spaces. J Glob Optim 1997;11:341–59.
[116] Sharma N, Anpalagan A. Differential evolution aided adaptive resource allocation in OFDMA systems with proportional rate constraints. Appl Soft Comput 2015;34:39–50.
[117] Muhsen DH, Ghazali AB, Khatib T, Abed IA. Extraction of photovoltaic module model's parameters using an improved hybrid differential evolution/electromagnetism-like algorithm. Sol Energy 2015;119:286–97.
[118] Ishaque K, Salam Z, Mekhilef S, Shamsudin A. Parameter extraction of solar photovoltaic modules using penalty-based differential evolution. Appl Energy 2012;99:297–308.
[119] Jiang LL, Maskell DL, Patra JC. Parameter estimation of solar cells and modules using an improved adaptive differential evolution algorithm. Appl Energy 2013;112:185–93.
[120] Gong W, Cai Z. Parameter extraction of solar cell models using repaired adaptive differential evolution. Sol Energy 2013;94:209–20.
[121] Zhang J, Sanderson AC. JADE: adaptive differential evolution with optional external archive. Evolut Comput IEEE Trans 2009;13:945–58.
[122] Kennedy J, Eberhart R. Particle swarm optimization. In: proceedings of IEEE international conference on neural networks. Perth, Australia; 1995, pp. 1942–48.
[123] Eberhart RC, Shi Y, Kennedy J. Swarm intelligence. United States: Elsevier; 2001.
[124] Rezaee Jordehi A, Jasni J. Parameter selection in particle swarm optimisation: a survey. J. Exp. Theor. Artif. Intell. 2013;25:527–42.
[125] Jordehi AR. A review on constraint handling strategies in particle swarm optimisation. Neural Comput Appl 2015:1–11.
[126] Jordehi AR, Jasni J. Particle swarm optimisation for discrete optimisation problems: a review. Artif Intell Rev 2013:1–16.
[127] Jordehi AR. Enhanced leader PSO (ELPSO): a new PSO variant for solving global optimisation problems. Appl Soft Comput 2015;26:401–17.
[128] Rezaee Jordehi A, Jasni J, Abdul Wahab NI, Kadir A, Abidin MZ. Particle swarm optimisation applications in FACTS optimisation problem. In: proceedings of the IEEE 7th international power engineering and optimization conference (PEOCO 2013). IEEE; 2013, p. 193–98.
[129] Jordehi AR, Jasni J. A comprehensive review on methods for solving FACTS optimization problem in power systems. Int Rev Electr Eng 2011;6.
[130] Alfi A. PSO with adaptive mutation and inertia weight and its application in parameter estimation of dynamic systems. Acta Autom Sin 2011;37:541–9.
[131] Khanna V, Das B, Bisht D, Singh P. A three diode model for industrial solar cells and estimation of solar cell parameters using PSO algorithm. Renew Energy 2015;78:105–13.
[132] AlRashidi M, AlHajri M, El-Naggar K, Al-Othman A. A new estimation approach for determining the I–V characteristics of solar cells. Sol Energy 2011;85:1543–50.
[133] AlHajri M, El-Naggar K, AlRashidi M, Al-Othman A. Optimal extraction of solar cell parameters using pattern search. Renew Energy 2012;44:238–45.
[134] Sahu RK, Panda S, Padhan S. A hybrid firefly algorithm and pattern search technique for automatic generation control of multi area power systems. Int J Electr Power Energy Syst 2015;64:9–23.
[135] Panda S, Kiran SH, Dash S, Subramani C. A PD-type Multi Input Single Output SSSC damping controller design employing hybrid improved differential evolution-pattern search approach. Appl Soft Comput 2015;32:532–43.
[136] Bouzidi K, Chegaar M, Nehaoua N. New method to extract the parameters of solar cells from their illuminated IV curve. In: proceedings of the 4th international conference on computer integrated manufacturing. Setif, Algeria; 2007, p. 1–4.
[137] Niu Q, Zhang L, Li K. A biogeography-based optimization algorithm with mutation strategies for model parameter estimation of solar and fuel cells. Energy Convers Manag 2014;86:1173–85.
[138] Ramesh Kumar A, Premalatha L. Optimal power flow for a deregulated power system using adaptive real coded biogeography-based optimization. Int J Electr Power Energy Syst 2015;73:393–9.
[139] Savsani P, Jhala RL, Savsani V. Effect of hybridizing Biogeography-Based Optimization (BBO) technique with Artificial Immune Algorithm (AIA) and Ant Colony Optimization (ACO). Appl Soft Comput 2014;21:542–53.
[140] Lohokare MR, Pattnaik SS, Panigrahi BK, Das S. Accelerated biogeography-based optimization with neighborhood search for optimization. Appl Soft Comput 2013;13:2318–42.
[141] Jordehi AR. Chaotic Bat Swarm Optimisation (CBSO). Appl Soft Comput 2014.
[142] Jordehi AR. Seeker optimisation (human group optimisation) algorithm with chaos. J Exp Theor Artif Intell 2015:1–10.
[143] Jordehi AR. A chaotic artificial immune system optimisation algorithm for solving global continuous optimisation problems. Neural Comput Applic 2014.
[144] Askarzadeh A, Rezazadeh A. Parameter identification for solar cell models using harmony search-based algorithms. Sol Energy 2012;86:3241–9.
[145] El-Naggar K, AlRashidi M, AlHajri M, Al-Othman A. Simulated Annealing algorithm for photovoltaic parameters identification. Sol Energy 2012;86:266–74.
[146] Lin S-W, Yu VF. A simulated annealing heuristic for the multiconstraint team orienteering problem with multiple time windows. Appl Soft Comput 2015;37:632–42.
[147] Wang J-C, Chen T-Y. A simulated annealing-based permutation method and experimental analysis for multiple criteria decision analysis with interval type-2 fuzzy sets. Appl Soft Comput 2015;36:57–69.
[148] Askarzadeh A, Rezazadeh A. Extraction of maximum power point in solar cells using bird mating optimizer-based parameters identification approach. Sol Energy 2013;90:123–33.
[149] Alam D, Yousri D, Eteiba M. Flower pollination algorithm based solar PV parameter estimation. Energy Convers Manag 2015;101:410–22.
[150] Yang X-S. Flower pollination algorithm for global optimization. In: Durand-Lose J, Jonoska N, editors. Unconventional computation and natural computation. Springer; 2012. p. 240–49.
[151] Bekdaş G, Nigdeli SM, Yang X-S. Sizing optimization of truss structures using flower pollination algorithm. Appl Soft Comput 2015;37:322–31.
[152] Draa A. On the performances of the flower pollination algorithm – qualitative and quantitative analyses. Appl Soft Comput 2015;34:349–71.
[153] Dizqah AM, Maheri A, Busawon K. An accurate method for the PV model identification based on a genetic algorithm and the interior-point method. Renew Energy 2014;72:212–22.
[154] Yuan X, Xiang Y, He Y. Parameter extraction of solar cell models using mutative-scale parallel chaos optimization algorithm. Sol Energy 2014;108:238–51.
[155] Niu Q, Zhang H, Li K. An improved TLBO with elite strategy for parameters identification of PEM fuel cell and solar cell models. Int J Hydrog Energy 2014;39:3837–54.
[156] Rao R, Savsani V, Vakharia D. Teaching–learning-based optimization: an optimization method for continuous non-linear large scale problems. Inf Sci 2012;183:1–15.
[157] Rao RV, Waghmare GG. Complex constrained design optimisation using an elitist teaching-learning-based optimisation algorithm. Int J Metaheuristics 2014;3:81–102.

[158] Yang D, Liu Z, Zhou J. Chaos optimization algorithms based on chaotic maps with different probability distribution and search speed for global optimization. Commun Nonlinear Sci Numer Simul 2014;19:1229–46.
[159] Yuan X, Yang Y, Wang H. Improved parallel chaos optimization algorithm. Appl Math Comput 2012;219:3590–9.
[160] Dkhichi F, Oukarfi B, Fakkar A, Belbounaguia N. Parameter identification of solar cell model using Levenberg–Marquardt algorithm combined with simulated annealing. Solar Energy 2014;110:781–8.
[161] Lera G, Pinzolas M. Neighborhood based Levenberg-Marquardt algorithm for neural network training. Neural Netw IEEE Trans 2002;13:1200–3.
[162] Petcut F-M, Leonida-Dragomir T. Solar cell parameter identification using genetic algorithms. J Control Eng Appl Inform 2010;12:30–7.
[163] Dragomir T, Petreuş D, Petcuţ F, Ciocan I. Comparative analysis of identification methods of the photovoltaic panel characteristics. In: proceedings of IEEE international conference on automation quality and testing robotics (AQTR 2010). IEEE; 2010. p. 1–6.
[164] Dali A, Bouharchouche A, Diaf S. Parameter identification of photovoltaic cell/module using genetic algorithm (GA) and particle swarm optimization (PSO). In: proceedings of the 3rd international conference on control, engineering & information technology (CEIT 2015). IEEE; 2015. p. 1–6.
[165] Jervase JA, Bourdoucen H, Al-Lawati A. Solar cell parameter extraction using genetic algorithms. Meas Sci Technol 2001;12:1922.
[166] Wei P, Yun Z, Hao G, Yong-qing L, Yong-hong Y, Wei H. Evolutionary algorithm and parameters extraction for dye-sensitised solar cells one-diode equivalent circuit model. Micro Nano Lett IET 2013;8:86–9.
[167] Appelbaum J, Peled A. Parameters extraction of solar cells – a comparative examination of three methods. Sol Energy Mater Sol Cells 2014;122:164–73.
[168] Moldovan N, Picos R, Garcia-Moreno E. Parameter extraction of a solar cell compact model usign genetic algorithms. In: proceedings of Spanish conference on electron devices, 2009 (CDE 2009). IEEE; 2009. p. 379–82.
[169] Ye M, Wang X, Xu Y. Parameter extraction of solar cells using particle swarm optimization. J Appl Phys 2009;105:094502.
[170] Hengsi Q, Kimball JW. Parameter determination of Photovoltaic Cells from field testing data using particle swarm optimization. In: proceedings of power and energy conference at illinois (PECI 2011). IEEE; 2011. p. 1–4.
[171] Jieming M, Ka Lok M, Ting TO, Nan Z, Sheng-Uei G, Wong PWH. Accelerating parameter estimation for photovoltaic models via parallel particle swarm optimization. In: proceedings of international symposium on computer, consumer and control (IS3C 2014); 2014. p. 175–178.
[172] Azab M. Identification of one-diode model parameters of PV devices from nameplate information using particle swarm and least square methods. In: First Workshop on Smart Grid and Renewable Energy (SGRE 2015). 2015. p. 1–6.
[173] Krishnakumar N, Venugopalan R, Rajasekar N. Bacterial foraging algorithm based parameter estimation of solar PV model. In: proceedings of annual international conference on emerging research areas and 2013 international conference on microelectronics, communications and renewable energy (AICERA/ICMiCR 2013). 2013. p. 1–6.
[174] Wei H, Cong J, Lingyun X, Deyun S. Extracting solar cell model parameters based on chaos particle swarm algorithm. In: proceedings of international conference on electric information and control engineering (ICEICE 2011). IEEE; 2011. p. 398–402.
[175] Ishaque K, Salam Z, Taheri H, Shamsudin A. A critical evaluation of EA computational methods for Photovoltaic cell parameter extraction based on two diode model. Solar Energy 2011;85:1768–79.
[176] Hachana O, Hemsas K, Tina G, Ventura C. Comparison of different metaheuristic algorithms for parameter identification of photovoltaic cell/module. J Renew Sustain Energy 2013;5:053122.
[177] Jacob B, Balasubramanian K, Azharuddin SM, Rajasekar N. Solar PV modelling and parameter extraction using artificial immune system. Energy Procedia 2015;75:331–6.
[178] Jacob B, Balasubramanian K, Babu TS, Rajasekar N. Parameter extraction of solar PV double diode model using artificial immune system. In: proceedings of IEEE international conference on signal processing, informatics, communication and energy systems (SPICES 2015); 2015. p. 1–5.
[179] Ishaque K, Salam Z. An improved modeling method to determine the model parameters of photovoltaic (PV) modules using differential evolution (DE). Solar Energy 2011;85:2349–59.
[180] Ismail M, Moghavvemi M, Mahlia T. Characterization of PV panel and global optimization of its model parameters using genetic algorithm. Energy Convers Manag 2013;73:10–25.
[181] Torres J, Guardado JL, Rivas-Dávalos F, Maximov S, Melgoza E. A genetic algorithm based on the edge window decoder technique to optimize power distribution systems reconfiguration. Int J Electr Power Energy Syst 2013;45:28–34.
[182] Suksonghong K, Boonlong K, Goh K-L. Multi-objective genetic algorithms for solving portfolio optimization problems in the electricity market. Int J Electr Power Energy Syst 2014;58:150–9.
[183] López-Lezama JM, Contreras J, Padilha-Feltrin A. Location and contract pricing of distributed generation using a genetic algorithm. Int J Electr Power Energy Syst 2012;36:117–26.
[184] Park J-Y, Choi S-J. Datasheet-based circuit parameter extraction method for maximum power point simulation of photovoltaic array. In: proceedings of the 9th international conference on power electronics and ECCE Asia (ICPE-ECCE Asia 2015). IEEE; 2015. p. 1413–19.
[185] Passino KM. Biomimicry of bacterial foraging for distributed optimization and control. Control Syst IEEE 2002;22:52–67.
[186] Naveen S, Sathish Kumar K, Rajalakshmi K. Distribution system reconfiguration for loss minimization using modified bacterial foraging optimization algorithm. Int J Electr Power Energy Syst 2015;69:90–7.
[187] Devi S, Geethanjali M. Application of modified bacterial foraging optimization algorithm for optimal placement and sizing of distributed generation. Expert Systh Appl 2014;41:2772–81.